Optimized MPPT implementation for Dye-sensitized Solar cells

Maximum Power Point Tracking for DCSs

KARTIK KARUNA

KTH Industrial Engineering and Management

Master's Degree Project
Stockholm, Sweden February 25, 2015

SAMMANFATTNING

KTH Industrial Engineering and Management

Examensarbete MMK 2014: MF212X

Optimized MPPT implementation for Dye-sensitized Solar cells

Kartik Karuna

Godkänt **2015-MM-DD**	Examinator **Martin Törngren**	Handledare **Baha Hasan**
	Uppdragsgivare **EXEGER Sweden AB**	Kontaktperson **Camila Niva**

(**Temp text not actual translation **) Europeiska kommissionens färdplan för ett utsläppssnålt samhälle kräver en drastisk minskning av användningen av kolbaserade bränslen. En ekonomi med låga koldioxidutsläpp skulle ha en mycket större behov av förnybara energikällor, energieffektiva byggmaterial och andra relaterade teknologier för att nå sina mål genom 2050. Mer lokalt producerad energi skulle användas, mestadels från förnybara källor med sol- och vinden spelar en allt större role.Energy effektivitet kommer att vara en viktig drivkraft för denna övergång. Designa själv-drivna enheter kan kompensera en stor del av kolet budgeten, vilket frigör enheter från att ta ut och göra dem riktigt trådlöst.

Färgsensibiliserade solceller eller Dye-sensitized solar cells (DSCs) på grund av deras låga kostnad tillverkningsteknik bland andra fördelar, kan mycket väl vara den saknade biten i detta pussel. Lägre effektivitet gentemot sin kiselbaserade motsvarigheter har dithered storskalig implementering, dock med fortsatt forskning som snart kommer att förändras. För att maximera den producerade energin, har flera spårning av maximal effektpunkt (maximum power point tracking,MPPT) algoritmer föreslagits och utvecklats under åren. De varierar i genomförandet, energieffektivitet, konvergens hastighet, sensorer krävs, kostnadseffektivitet etc. Även jämförande studier, baserade på allmänt antagna MPPT algoritmer, har presente tidigare fokuserat på kommersiellt tillgängliga Silicon baserade Solar-celler; ingen har tillämpat sina iakttagelser till DSCs inomhus förhållanden. Detta arbete presenterar en experimentell jämförelse under simulerad inomhus bestrålning, av tre mest använda MPPT metoder för PV kraftsystem i ett försök att hitta en som passar bäst för DSCs. Efterföljande experiment visade de existerande MPPT metoder för att vara olämpliga för DSCs som leder till en ny hybrid algoritm föreslås.

Nyckelord: DSCs, Grätzel cells, MPPT, PnO, INC, Golden sökalgoritm, Maskininlärning.

ABSTRACT

KTH Industrial Engineering and Management

Master of Science Thesis MMK 2014: MF212X

Optimized MPPT implementation for Dye-sensitized Solar cells

Kartik Karuna

Approved **2015-MM-DD**	Examiner **Martin Törngren**	Supervisor **Baha Hasan**
	Commissioner **EXEGER Sweden AB**	Contact person **Camila Niva**

European Commission's roadmap for moving to a low-carbon economy calls for a drastic reduction in the use of carbon based fuels. A low-carbon economy would have a much greater need for renewable sources of energy, energy-efficient building materials and other related technologies in order to reach goals by 2050. More locally produced energy would be used, mostly from renewable sources with solar and wind playing an ever increasing role.Energy efficiency will be a key driver of this transition. Designing self-powered devices could offset a huge portion of the carbon budget, freeing devices from charging and making them truly wireless.

Dye-Sensitized Solar Cells (DSCs) owing to their low-cost manufacturing technique among other advantages, could well be the missing piece in this puzzle. Lower efficiency vis-à-vis its Silicon based counterparts have dithered large scale implementation, however, with continued research that is soon to change. In order to maximize the produced energy, several maximum power point tracking (MPPT) algorithms have been proposed and developed over the years. They vary in implementation, energy efficiency, convergence speed, sensors required, cost effectiveness etc. Although comparative studies, based on widely-adopted MPPT algorithms, have been presented before they focused on commercially available Silicon based Solar-cells; none have applied their findings to DSCs in indoor conditions. This work presents an experimental comparison, under simulated indoor irradiation, of three most used MPPT methods for PV power systems in an attempt to find one most suitable for DSCs. Subsequent experiments showed the existing MPPT methods to be unsuitable for DSCs leading to a new hybrid Algorithm being proposed.

Keywords: DSCs,Grätzel cells, MPPT, PnO, INC, Golden Search Algorithm, Machine Learning.

ACKNOWLEDGMENTS

This thesis has been conducted at EXEGER Sweden AB in Stockholm with support from KTH- The Royal Institute of Technology, between the months of January and November of 2014. I would like to acknowledge all the people and institutions that have contributed directly and indirectly to this work.

First of all, I would like to express my gratitude to my manager Dr.Camilla Niva for being extremely patient, understanding and for her constant encouragement all through my period here. To Mr.Giovanni Fili, CEO and Dr.Henrik Lindström, CTO; for providing me with this extraordinary opportunity of completing my studies while working at EXEGER.

I would like to extend my thanks to Dr.Martin Törngren, for this thesis would be incomplete without his invaluable guidance and critique. A special thanks to Baha Hasan, my supervisor at KTH, who provided me with insightful advice and support.

I am also grateful to my colleagues Dr.Jarl Nissfolk, Dr.Magdalena Marszalek and Mikael Källberg. They provided rich insights into their respective fields of expertise and contributed to a conducive atmosphere for research.

last but not least, to my wife Harita, who put up with my extremely odd working hours, kept me in good spirits and for being by my side for everything, always.

Kartik Karuna,
Stockholm, November 2014.

CONTENTS

LIST OF FIGURES

ACRONYMS

DSCs	Dye-Sensitized Solar Cells	1
MPPT	Maximum Power Point Tracking	1
CdTe	Cadmium telluride	1
CIGS	Copper-indium-gallium selenide	1
CIS	Copper-indium sulphide	1
a-Si	Amorphous silicon	1
FTO	Fluorine-doped tin oxide	9
WE	Working Electrode	9
CE	Counter Electrode	9
HOMO	Highest Occupied Molecular Orbital	10
LUMO	Lowest Unoccupied Molecular Orbital	10
MPP	Maximum Power Point	3
PnO	Perturb and Observe	6
FOCV	Fractional Open Circuit Voltage	6
ICM	Incremental Conductance Method	6
F.F	Fill Factor	12
SMU	Source-Measure Unit	29
DSP	Digital Signal Processor	44
VAL	Voltage approximation line	44
LED	Light Emitting Diode	27

1 INTRODUCTION

This chapter gives a basic introduction to Dye-Sensitized Solar Cells (DSCs) and Maximum Power Point Tracking (MPPT).It also defines the Scope, Goals, Objective and the Research methodology for the thesis.

1.1 BACKGROUND

Our ever increasing reliance on electrical and electronic equipment intensified our search for new sources of energy. Dwindling fossil-fuel reserves are not something we can rely on in the long-term. Alternate energy sources must be efficient, cost-effective and ecologically friendly. The harnessing of solar energy becomes a very attractive proposition. A moderately efficient solar cell array (8% - 10% efficiency) covering a small portion of the earth's surface would be able to provide an enormous amount of electric power and thus reduce greenhouse-gas emissions [18]. However, the current high cost of solar panels made from traditional inorganic semiconductors imposes a restriction on their mass usage. **picture about the losses Solar energy intercepting Earth [toivola2010dye]**

1.1.1 Dye-Sensitized Solar Cells(DSCs)

Photovoltaic devices are based on the concept of charge separation at an interface of two materials of different conduction mechanism. To this date, the field has been dominated by Solid-state junction devices, usually made of silicon, and profiting from the experience and material availability resulting from the semiconductor industry. The dominance of the photovoltaic field by inorganic Solid-state junction devices is now being challenged by the emergence of a third generation of cells, based on nano-crystalline oxide and conducting polymer films [13]. Crystalline silicon being the first; and thin film technologies such as Cadmium telluride (CdTe), Copper-indium-gallium selenide (CIGS), Copper-indium sulphide (CIS) and Amorphous silicon (a-Si) being examples of the second generation [28].

Solar energy can be converted into electricity by a variety of technologies that can also be divided into four classes: Concentrator systems, wafer-based crystalline silicon, thin-film technologies and emerging technologies[32].

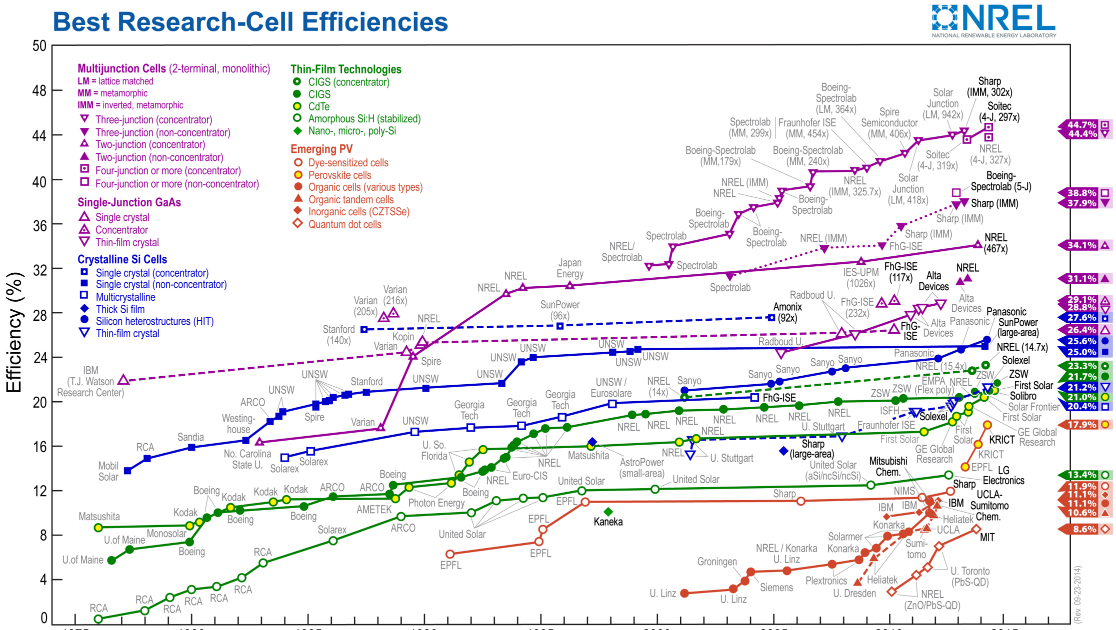

Figure 1.1: Research Cell Efficiency Records [24]

Dye-sensitized solar cells(DSCs) are the most promising of the third and latest generation of solar cells. Under development for the last 20 years, this technology is ready for large scale commercialization to provide robust, efficient and affordable solar energy to the masses. Unlike previous generation cells, DSCs is a Photo-electro-chemical device whose principle of operation is similar to Photosynthesis seen in plants.

1.1.2 Advantages of DSCs

The rate of adoption for solar cells is slow. A major contributing factor for this is the predominant type of solar cells used today -ones made from silicon, which are quite expensive and are complex to manufacture. This has lead to intensive research into alternative solar cells in the past decade. DSCs have many advantages over their 1st and 2nd generation counterparts. They offer transparency, low cost, and high power conversion efficiencies under cloudy and artificial light conditions.DSCs work even in low-light conditions such as non-direct sunlight and cloudy skies.They are easy and economical to manufacture,with the major constituent materials available in abundance in most counties. This copious availability of raw material also enables us to scale the manufacturing to Tera-Watt levels with relative ease. Raw-materials are non-toxic and there are no noxious emissions during fabrication - leading to sustainable manufacturing.

		Performance			
		World record efficiency	Module efficiency	Sensitivity to light angle and condition	Sensitivity to temperature fluctuations
1st generation PV	Mono-crystalline silicon	30.0%	19.5%	High	- 0.53% / °C
	Multi-crystalline silicon	18.0%	13.0-15.0%	High	- 0.44% / °C
2nd generation PV	Cadmium telluride	17.3%	13.5%	Medium	- 0.27% / °C
	CIGS	20.3%	15.1%	Medium	- 0.42% / °C
	Amorphous silicon	13.0%	5.0-7.0%	Medium	- 0.20% / °C
3rd gen.	DSCs	14.14% (15%)	10.3%	Low	+ 0.1% / °C

Figure 1.2: Three generations of cells – Performance

**Add more details about Advantage of DSC over conventional cells **

1.2 MAXIMUM POWER POINT TRACKING(MPPT)

A Photo-Voltaic (PV) array that functions under uniform radiation and temperature conditions presents an I–V and P–V characteristic as the one shown in Figure 1.3 and Figure 1.5,respectively. As can be observed, there is a single point, called Maximum Power Point (MPP), where the array provides the maximum power possible for these environmental conditions (radiation and temperature), and so functions with the maximum performance. When a load is connected directly to a PV array (direct coupling), the operation point is defined by the intersection of its I–V characteristics, as shown in Figure 1.3. In general, this operation point does not coincide with the MPP. Thus, in direct coupling systems, the array must be over-dimensioned to guarantee the power demand of the load. Obviously, this implies a more expensive system. To solve this problem, a DC/DC converter with an algorithm for the automatic control of its duty cycle "δ" is inserted between the photovoltaic array and the load , resulting in what is known as MPPT system. The MPPT must control the voltage or current (through the δ the converter) of the PV array regardless of the load, trying to place it in the MPP.Therefore,the MPPT must find the optimal δ for the operation point of the PV array to coincide with the MPP[6].

Although the solution to operating in the MPP may seem straightforward, it is not!

This is because the location of the MPP in the I–V curve of the PV array is not known beforehand. This point must be located, either by mathematical calculations over a valid model, or by using some search algorithm. This implies even more difficulty if we consider the fact that the MPP presents non-linear dependencies with temperature and radiation[6]

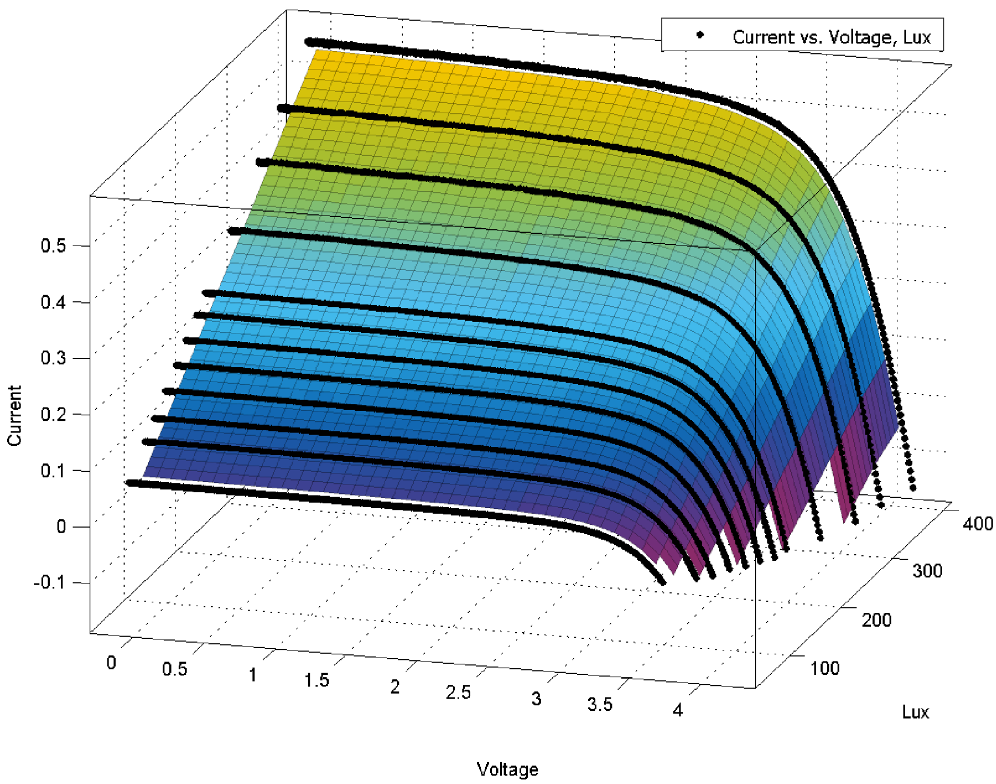

Figure 1.3: I-V-Lux

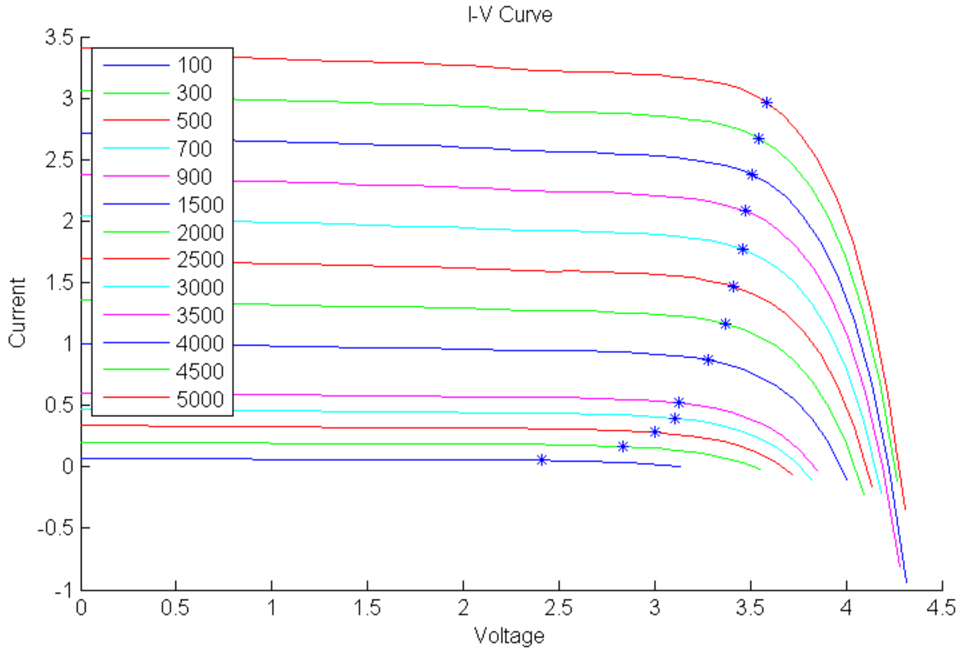

Figure 1.4: I-V Graph, MPPT marked with '*'

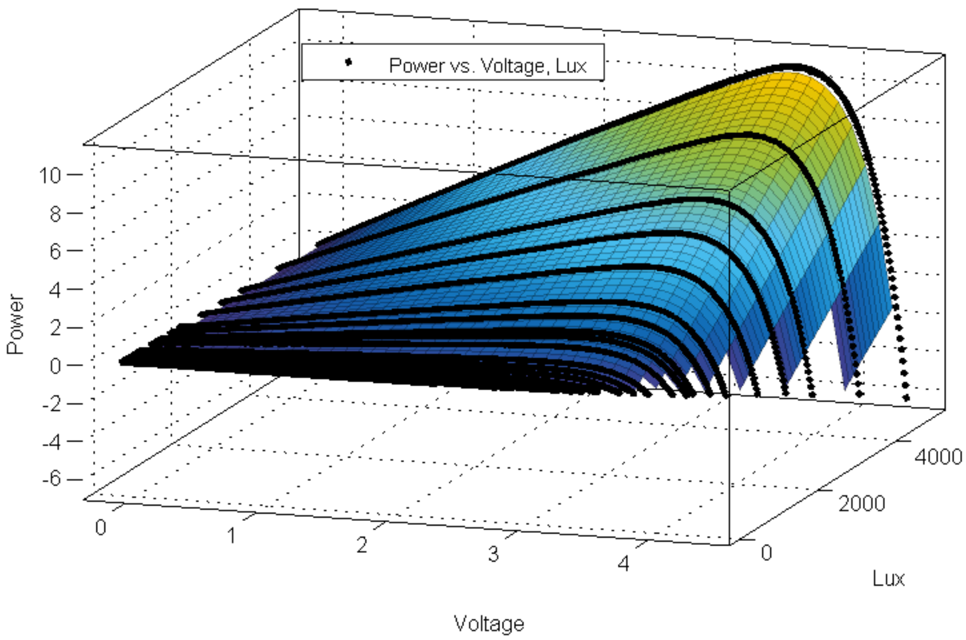

Figure 1.5: P-V Lux

As such, numerous MPPT methods have been developed and implemented[23] [7] [5] . The methods vary in complexity, sensors required, convergence speed, cost, range of effectiveness, implementation hardware, popularity, and in other respects[25] [4]. They range from the almost obvious (but not necessarily ineffective) to the most creative (not necessarily most effective). In fact, so many methods have been developed that it has become difficult to adequately determine which method, newly proposed or existing, is most appropriate for a given PV system.Some of the most popular being:

- Perturb and Observe Method
- Incremental Conductance Method
- Fractional Open Circuit Voltage Method
- Fixed duty cycle Method
- Pilot Cell Method
- Fractional short-circuit current Method
- Fuzzy-logic controller

1.3 SCOPE, THESIS GOALS AND OBJECTIVES

This thesis focuses on the finding a practical and usable MPPT algorithm that is optimised to be used with current DSCs.

The objectives of the thesis can be summarized as:

- Develop an electrical model for DSCs and verify the accuracy of said model.
- Compare and optimise the following Maximum Power Point Tracking (MPPT) algorithms for compatibility with the above Model using MATLAB® and Simulink®.
  1. Perturb and Observe (PnO) Method.
  2. Incremental Conductance Method (ICM).
  3. Fractional Open Circuit Voltage (FOCV) Method.
- Setting up the test environment
- Execution of test cases on prototype developed, based on two of the best optimised algorithms, with recordable test results.
- Develop reference designs for production.
- Internal report.
- Master thesis report.

1.4 THESIS OUTLINE

- Chapter 1 Presents the background and the main objectives of this thesis.
- Chapter 2 Contains the prior research and literature that this thesis was based on. It also discusses the operating principles/state-of-the-art of DSCs and of MPPT.
- Chapter 3 Concerns the research methods, measurement techniques and implementation of the thesis.
- Chapter 4 Gives a summary of the results.
- The thesis is concluded and future work talked about in Chapter 5.

1.5 RESEARCH METHODOLOGY

The implementation of the thesis is the four steps.

- Develop a suitable model for the DSCs based on either:
  1. the single diode equation for DSCs.
  2. based on experimental modelling methods .
- Objective study of current algorithms; weigh their advantages against their flaws.
- Validation of the model and algorithm in MATLAB® and Simulink®.
- Implementation in test Hardware .

2 RELATED LITERATURE

This section explores contemporary academic/scientific papers and articles that establish the research context necessary for the thesis.

2.1 DYE-SENSITIZED SOLAR CELLS(DSCS)

The basic structure of DSCs is represented in the Figure 2.1.

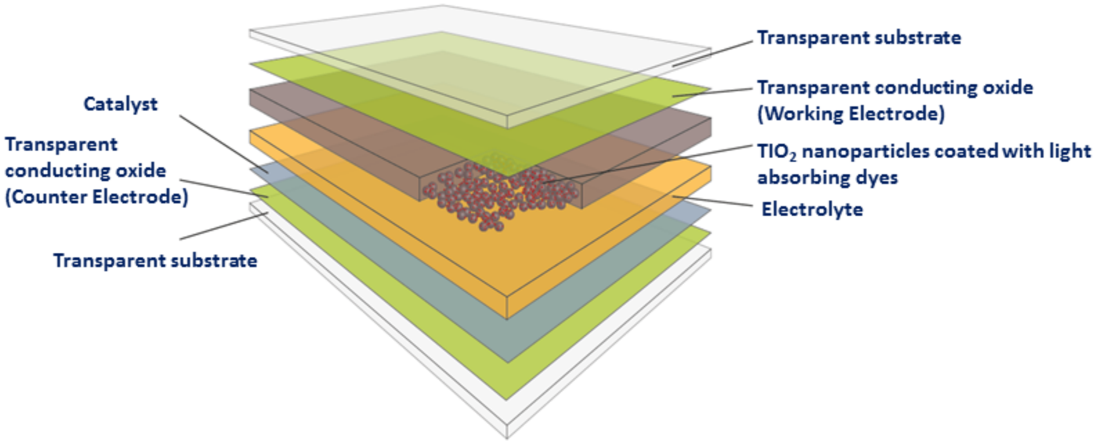

Figure 2.1: Structure of a DSC

The most commonly used substrate is glass coated with Fluorine-doped tin oxide (FTO). Attached to the surface of the nano-crystalline particles of Titanium dioxide(TiO_2) is a mono-layer of the light-sensitive-charge-transfer dye. The dye absorbs photons of incoming light and uses this energy to release free electrons to the TiO_2 layer acting as the Working Electrode (WE) and then onto metal contacts. An electrolyte is filled between the electrodes and helps transfer electrons from the Counter Electrode (CE) to the dye particle (which is in an oxidised state due to a loss of electron) to reduce it back to its ground state. The most commonly used redox couple and the one that gives the best cell efficiencies when combined with TiO_2, is iodide/triiodide (I^-/I_3^-). The oxidised dye gets electrons from the iodide ions which, in turn, get oxidised to triiodide in the process. The triiodide ions then diffuse to the counter electrode, where they get reduced back to iodide by the electrons returning from the external load. Thus, the cell operation is based on consecutive reduction/oxidation cycles and, in an ideal cell, no chemical substances are permanently transmuted. The most often used counter electrode catalyst for the triiodide/iodide reduction reaction is platinum, though also carbon materials and certain conductive polymers have been successfully employed in this function.

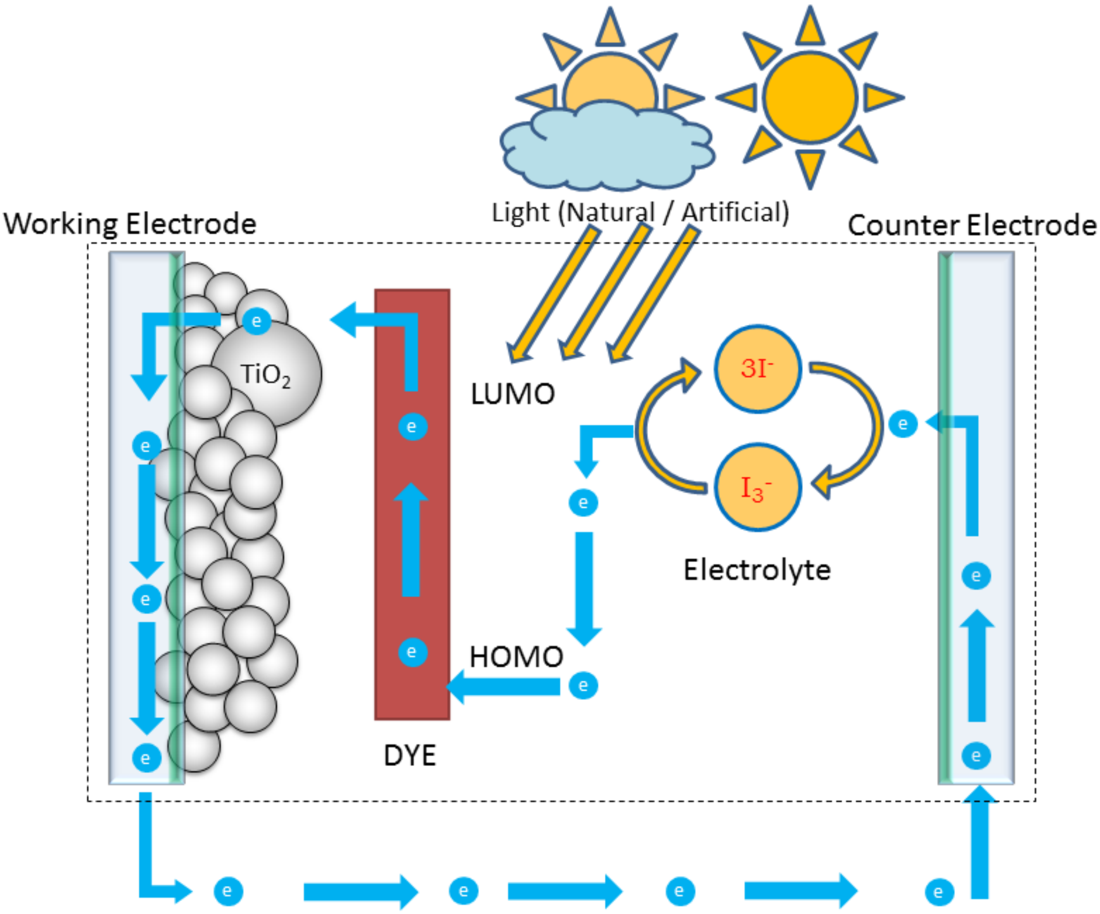

Figure 2.2: The structure and operating principle of a DSC (adapted from [28][10])

The amount of current that the cell is able to generate is determined by the energetic distance of the Highest Occupied Molecular Orbital (HOMO) and Lowest Unoccupied Molecular Orbital (LUMO) of the dye, which equals the band gap in inorganic semiconductors. The maximum voltage, on the other hand, is defined as the difference between the redox level of the electrolyte and the Fermi level of the TiO_2.With iodide/triiodide redox couple, this difference is 0.9 V, though slight variation is caused by the electrolyte composition due to species adsorbed on the TiO_2 surface, which may somewhat alter the Fermi level position. Also, there is always some recombination in the cell which lessens the amount of electrons in the TiO2 film, thus lowering the Fermi level and decreasing the cell voltage. [28]. This operating principle of DSCs is depicted in the Figure 2.2 on page 10.

2.1.1 Single diode model

The simplest equivalent circuit of a generic solar cell is a Single diode model comprising of a current source in parallel with a diode.A slightly more detailed model includes a shunt resistance of the cell which takes into account the parallel resistive losses representing leakage current across the junction in the cell. This model is sometimes referred to as a single exponential five-parameter model[31]. The incident photons induces a current in the active area that is proportional to the intensity of the light falling on the cell.

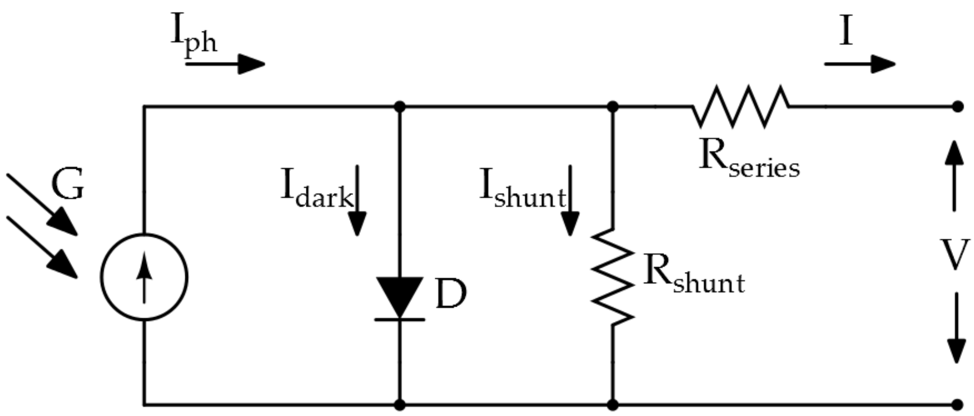

Figure 2.3: Single diode model for a solar cell

The power conversion efficiency of a solar cell is determined from the current versus applied voltage (I-V) characteristics under illumination. The I-V curve and device efficiency are reported with respect to a standard reference spectral irradiance distribution, the air mass 1.5 global (AM 1.5G) spectrum[32]. The I-V characteristics of a solar cell are well described by an equivalent electric circuit in Figure 2.3 on page 11 . Under illumination, a constant photo current (I_{ph}) is generated. If a forward voltage bias is applied, a dark diode current (I_{dark}) flows in the opposite direction. A shunt resistance (R_{shunt}) may arise from charge recombination in the photo-active layer and induce a shunting current(I_{shunt}).The series resistance (R_{series}) includes the contact resistance at interfaces, the bulk resistance and the sheet resistance of the transparent electrodes. The total measured current then is:

$$I = I_{ph} - I_{dark} - I_{shunt} = I_{ph} - I_s(e^{\frac{eV}{mkT}} - 1) - \frac{V + IR_{series}}{R_{shunt}} \tag{2.1}$$

where $\mathbf{I_s}$ is the diode saturation current, **V** is the applied bias voltage, ***m*** is an ideality factor ($m = 1$ for an ideal cell), ***k*** is the Boltzmann constant, and **T** is the device temperature[32]. For small forward bias voltages the numerical value of the exponential is very large and the thermal voltage very small, therefore the '-1' in the diode equation can be safely neglected and the forward diode current can be written as[14]:

$$I_{dark} = I_s(e^{\frac{eV}{mkT}}) \tag{2.2}$$

Substituting the value of I_{dark} back in equation 2.1 and neglecting the shunt resistance we can simplify the equation to as below (equation 2.3). This can be schematically depicted as Figure 2.4 on page 12. The simplified equation suffices for most modelling applications.

$$I = I_{ph} - I_{dark} - I_{shunt} = I_{ph} - I_s(e^{\frac{eV}{mkT}}) \tag{2.3}$$

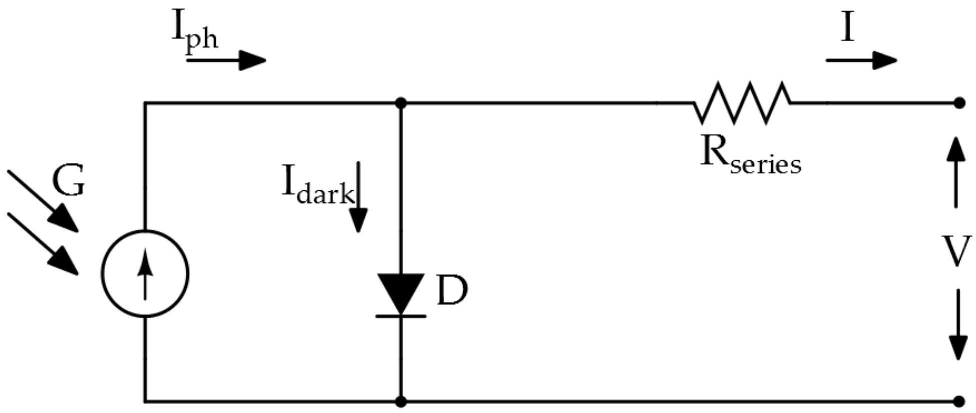

Figure 2.4: Simplified single diode model for a solar cell

The maximum-power operating point defines the condition at which the power output (P_{max} = $I_{max}V_{max}$) of the device is maximal. The so-called Fill Factor (F.F) is often used to characterise the maximum power ,

$$F.F = \frac{I_{max}V_{max}}{I_{sc}V_{oc}} \tag{2.4}$$

The accuracy and complexity of the model can be increased by including Temperature dependence of the photo current and diode saturation current; shunt resistance in parallel with the diode and accommodating for variance in the quality factor of the diode either by having a variable parameter or introduction of an additional diode into the circuit as done in the Double Diode Model.

2.1.2 Double diode model

The single diode equation assumes a constant value for the ideality factor n. In reality, the ideality factor is a function of voltage across the device. At high voltages, when the recombination in the device is dominated by the surfaces and the bulk regions, the ideality factor is close to one. However at lower voltages, recombination in the junction dominates and the ideality factor approaches two. The junction recombination is modelled by adding a second diode in parallel with the first and setting the ideality factor typically to two(ideality factor, n for $D_1 = 1$ and $D_2 = 2$)[14].

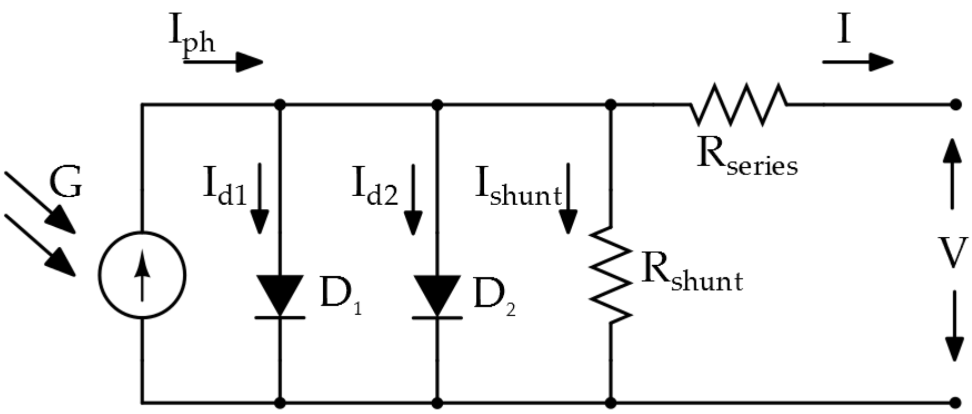

Figure 2.5: Double diode model for a solar cell (adapted from [14])

The equation of the double diode model under illumination is given by:

$$I = I_{ph} - I_{dark} - I_{shunt} = I_{ph} - I_{s1}(e^{\frac{eV}{kT}} - 1) - I_{s2}(e^{\frac{eV}{2kT}} - 1) - \frac{V + IR_{series}}{R_{shunt}} \tag{2.5}$$

2.1.3 Equivalent DSCs model

It has normally been found that DSCs do not conform to the typical I-V curves obtained from transmission line model and ladder circuit[33]. DSCs are often modelled with circuits similar to conventional *pn*-junction solar cell (Section 2.1.1 and 2.1.2), however even these representations fail to correspond to experimentally obtained values.

A standard DSCs typically contains three interfaces formed by FTO/TiO_2, TiO_2/dye/ electrolyte, and electrolyte/Pt-FTO as depicted in the Figure 2.2 on page 10. The equivalent circuit below (Figure 2.6) accounts for these interfaces. The interfacial charge transfer at the TiO_2/ dye/ electrolyte is represented by a rectifying diode(D_1) and a double-layer capacitance (C_i). A recombination diode D_2 is employed to denote the interfacial charge recombination losses to both the dye cation and the redox electrolyte. Parallel resistive losses across the cell including leakage current is indicated by R_{Shunt}. The photo-generated current I_{ph} is in parallel with the diodes and C_i. An inductive recombination pathway as a result of a charge-transfer current is incorporated into the circuit, consisting of a recombination resistance (R_{rec} in series with the an inductor (L). The charge-transfer resistance and interfacial capacitance at the FTO electrode and electrolyte/Pt-FTO interface are represented by R_E and C_E, and R_{CE} and C_{CE} respectively. The Nernst diffusion of the carrier transport by ions within the electrolyte is denoted by the Warburg impedance (W). A resistance element R_{Series}, designates the bulk and contact resistive losses present in a practical DSCs, such as the sheet resistance of the FTO glass, contact resistance etc. The I-V characteristics based on the equivalent circuit model in figure 2.6 is described in equations 2.6 [33].

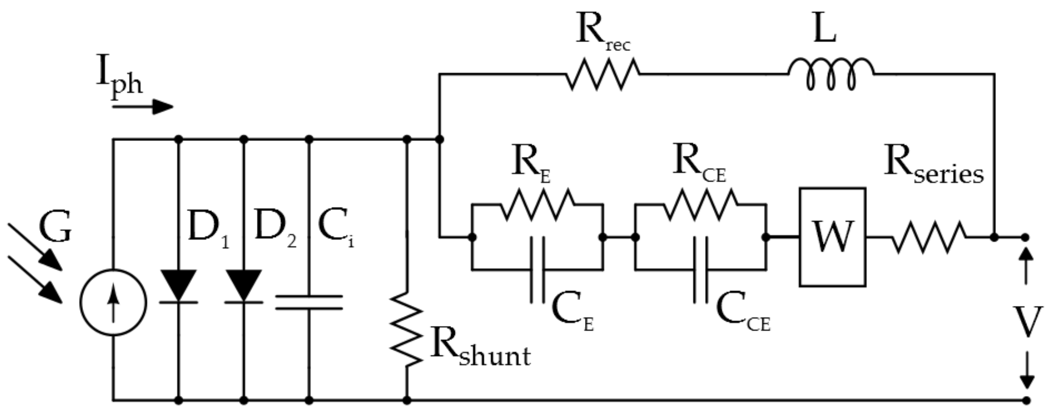

Figure 2.6: Equivalent circuit for DSCs (adapted from [33])

$$I = I_{ph} - I_{s1}(e^{\frac{eV}{mkT}} - 1) - I_{s2}(e^{\frac{eV}{2mkT}} - 1) - (V + IZ)(j\omega C_i + \frac{1}{R_{Shunt}}) \tag{2.6}$$

$$I_{ph} = \int qF(\lambda)[1 - r(\lambda)]IPCE(\lambda)d\lambda = \int qF(\lambda)\Phi(\lambda)d\lambda \tag{2.7}$$

$$Z = \frac{1}{\frac{1}{(R_{rec} + j\omega L)} + \frac{1}{Z_S}} \tag{2.8}$$

$$Z_S = \frac{1}{j\omega C_E + \frac{1}{R_E}} + \frac{1}{j\omega C_{CE} + \frac{1}{R_{CE}}} + W + R_S \tag{2.9}$$

$$W = \sigma\omega^{-1/2}(1 - j) \tag{2.10}$$

Where T is the absolute temperature, ω is the angular frequency, σ is the Warburg coefficient, $F(\lambda)$ and $IPCE(\lambda)$ are the incident photon flux density and the incident photon-to-current conversion efficiency at wavelength λ respectively, $r(\lambda)$ is the incident light losses due to the light absorption and reflection by the FTO glass, and $\Phi(\lambda)$ is the quantum yield [33].

2.2 MAXIMUM POWER POINT TRACKING(MPPT)

Despite all the advantages presented by the generation of energy through the use of solar cells the efficiency of energy conversion is currently low (the best commercial solar module is only 21.5% efficient) and the initial cost for its implementation is still considered high. Thus it becomes pertinent to use various techniques to extract the maximum power from these cells, in order to achieve maximum efficiency in operation. It should be noted that there is only one maximum power point (MPP) for a given panel, and this varies according to climatic and irradiation conditions[5].

To overcome this problem, several methods for extracting the maximum power have been proposed and many comparative studies have been published in literature [23],[7],[5],[25]and [8].

2.2.1 Perturb and Observe (PnO) Method

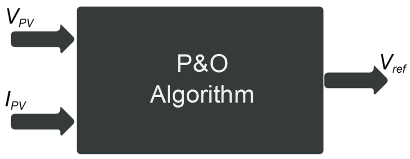

Figure 2.7: Black box model for the Perturb and Observe Algorithm

The PnO Method is most widely used in MPPT because of its simple structure and it requires only few parameters. Figure 2.8 shows the flow chart of PnO method. It perturbs the PV array's terminal voltage periodically and then it compares the PV output power with that of the previous cycle of perturbation. When PV power and PV voltage increase at the same time and vice versa, a perturbation step size, ΔD will be added to the duty cycle, D to generate the next cycle of perturbation in order to force the operating point moving towards the MPP. When PV power increases and PV voltage decreases and vice versa, the perturbation step will be subtracted for the next cycle of perturbation. This process will be carried on continuously until MPP is reached. However, the system will oscillate around the MPP throughout this process, and this will result in loss of energy. These oscillations can be minimised by reducing the perturbation step size but it significantly slows down the MPP tracking system also leading to loss of energy [23]. PnO is also not suitable when the light intensity changes rapidly.

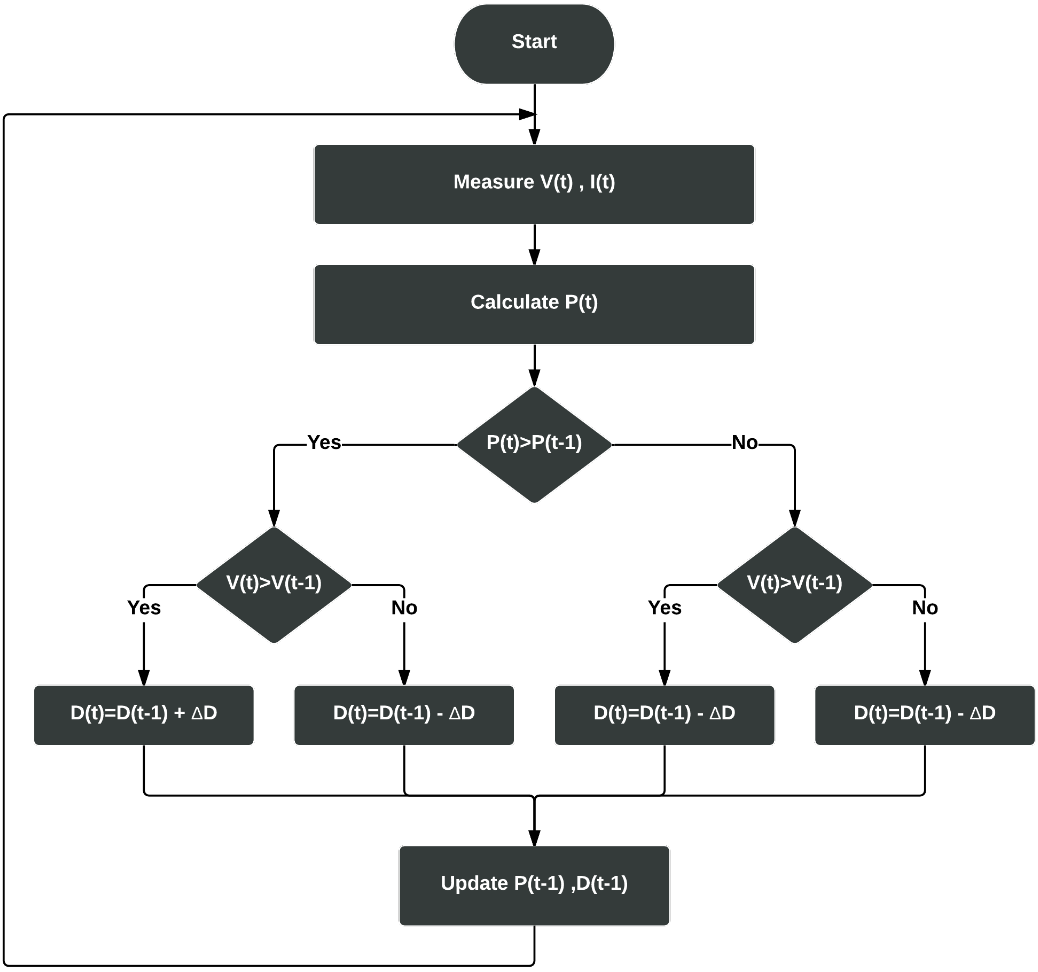

Figure 2.8: Flow chart for the Perturb and Observe Method

2.2.2 Incremental Conductance Method (ICM)

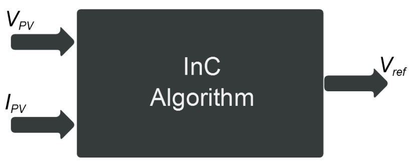

Figure 2.9: Black box model for the Incremental Conductance Algorithm

The solar array terminal voltage can be adjusted relative to the MPP voltage by measuring the incremental and instantaneous array conductance (dI/dV and I/V, respectively). The algorithm is based on the fact that at the MPP, the derivative of the cell's power is zero. Although the incremental conductance method offers good performance under rapidly changing atmospheric conditions, four sensors are required to perform the computations. The drawback is that sensor devices require more conversion time thus resulting in a large amount of power loss [12]. In addition to the above drawback, the ICM suffers the same limitations as PnO method namely, for rapid tracking larger step sized must be utilised which results in the oscillation around the MPP.

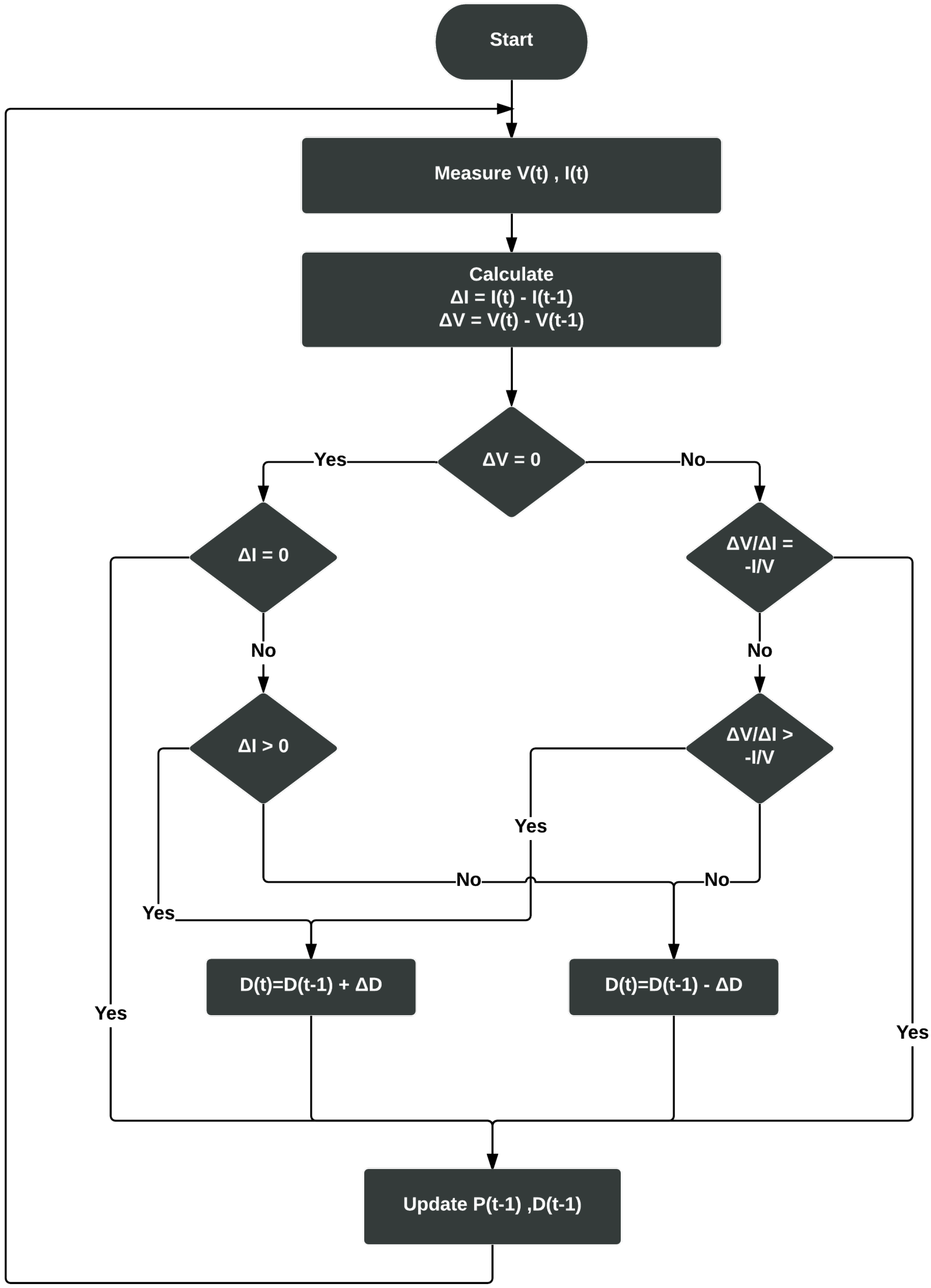

Figure 2.10: Flow chart for the Incremental Conductance Method

2.2.3 Fractional Open Circuit Voltage (FOCV) Method

Figure 2.11: Black box model for the Incremental Conductance Algorithm

This is a method based on the linear relationship between output voltage of the PV array at the MPP, V_{MPP} and the PV array's open circuit voltage, V_{OC} in under varying temperature and solar irradiance.

$$V_{MPP} \approx k_i V_{OC} \tag{2.11}$$

Constant value of k_i is dependent on the characteristics of PV array. Generally, it has to be computed empirically in order to determine the V_{MPP} and V_{OC} for varied temperatures and solar irradiances. The value of k_i ranges from 0.73 to 0.80 for most PV modules over a temperature range of 0 to 60°C.Figure 2.12 describes the operation of a FOCV, the PV array is temporarily isolated from MPPT,then the open circuit voltage, V_{OC} is measured periodically by shutting down the power converter momentarily. The MPPT calculates V_{MPP} from the pre-set value of k_i and the calculated value of V_{OC}. Then, the array's voltage is varied until V_{MPP} is reached . The shut-down of power converter periodically will incur temporary loss of power which in turn leads to a situation where power extracted will not be the maxima. Since it is an approximation, the PV array will never reach the MPP. Even though this technique is very easy and cheap for implementation; due to the fact true MPP is never reached, there is always a loss in power during operation[23].

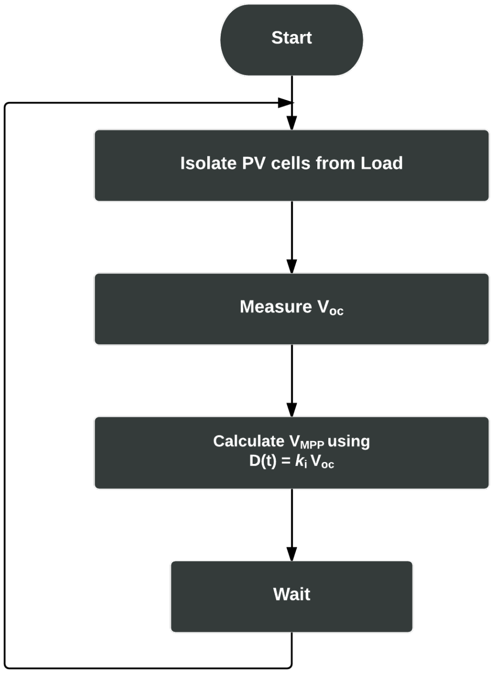

Figure 2.12: Flow chart for the Fractional Open Circuit Voltage Method (adapted from [25])

2.2.4 Other algorithms

- **Fixed duty cycle**: The fixed duty cycle represents the simplest of the methods and it does not require any feedback, where the load impedance is adjusted only once for the maximum power point and it is not adjusted again.
- **Pilot cell**: In the pilot cell MPPT algorithm, the constant voltage or current method is used, but the open-circuit voltage or short-circuit current measurements are made on a small solar cell, called a pilot cell, that has the same characteristics as the cells in the larger solar array. The pilot cell measurements can be used by the MPPT to operate the main solar array at its MPP, eliminating the loss of PV power during the V_{OC} or I_{sc} measurement
- **Fractional short-circuit current** : Under varying atmospheric conditions, I_{MPP} is approximately linearly related to the I_{SC} of the PV array.

$$I_{MPP} \approx k_j I_{SC} \tag{2.12}$$

- **Fuzzy logic controller** (FLC):They have the advantages of working with imprecise inputs, it does not need an accurate mathematical model and it can handle non-linearity as well [22].However their effectiveness depends a lot on the presence of an expert knowledge; conversely, in the absence of such knowledge, their design is usually slow and not optimised.

2.3 MACHINE LEARNING

This section discusses about Search optimization in order to lock on the V_{MP} and I_{MP} as efficiently as possible.

Much like Embedded systems, Machine Learning encompasses various disciplines, predominantly Computer science but also statistics, Mathematics, Finance etc. [21]; with applications ranging from predicting emergency-room wait-times [3] to High Frequency Stock-trading. Simply put, Machine learning is about algorithms that build models which adapt or modify their response in order to get closer to the correct output. These models are automatically created and they constantly evolve based on input vectors, as opposed to having a hard coded decision tree.

If the input vectors provided to the algorithm in its training set are 'labelled' , then this kind of learning is called **Supervised learning**. Where correct or expected responses are provided based on this the algorithm is able to generalise the out put for all possible outputs. In the other end of the spectrum is **Unsupervised learning** in which the algorithm is left to find hidden structures in a set of data that doesn't have any labels or that all have the same label. In our application we know the input is V_{OC} and what the expected Output (V_{MPP})is supposed to be. This constitutes as labelling and hence classified as Supervised learning.

2.3.1 Regression Modelling

We use regression analysis when we want to predict one variable from another. The most basic form of regression is called simple regression, where one independent variable and one dependent variable exists and where linear trend is to be predicted. In regression, we attempt to determine the magnitude of the relationship between a set of independent variables and the dependent variable. Independent variable(X), also called the predictor variable, influences the Dependent variable(Y),sometimes called the response variable [27].

A regression model is a formal way of stating:

- The tendency of the response variable(Y) to vary with the predictor variable(X).
- A scattering of points around some statistical relationship.

Equation for a line can be written as:

$$y = mx + b \tag{2.13}$$

The linear regression model(for observation i = 1, . . . , N) can we written as:

$$Y_i = \beta_0 + \beta_1 X_i + \epsilon_i \tag{2.14}$$

- β_0 is the mean of the population when X is zero -the Y intercept.

- β_1 is the slope of the line, the amount of increase in Y brought about by a unit increase $(X' = X + 1)$ in X.
- ϵ_i is the random error, specific to each observation.
- the goal is to find β_0 and β_1 such that $\sum_{i=1}^{n} \epsilon_i{}^2$ is minimised.

A large number of methods and procedures have been developed to estimate the parameters of a model, the simplest being :

$$\beta_1 = \frac{\sum(X_i - \bar{X})(Y_i - \bar{Y})}{\sum(X_i - \bar{X})^2} \tag{2.15}$$

$$\beta_0 = \bar{Y} - \beta_1 \bar{X} \tag{2.16}$$

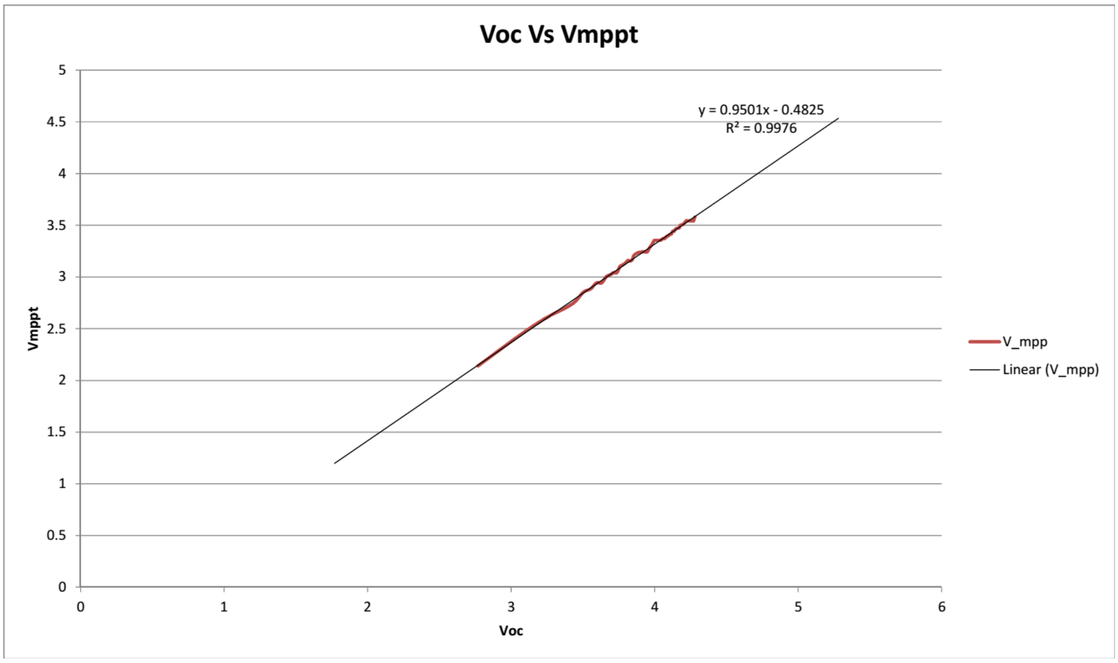

Figure 2.13: Example for Linear regression

In Figure 2.13 the points in red represent V_{MPP} for a given V_{OC}. It is clear from the graph that the relationship between V_{MPP} and V_{OC} is linear, this is also supported in various literature ([25],[7],etc.) and forms the basis of FOCV method. The trend line in black (obtained via Regression Modelling) tells us about the slope of the line (β_1) and the Y intercept. It also provides the R^2 value of the fit equal to 0.9976, indicating the goodness of fit. R^2 is a measure of how close the regression line is to the data points, with $R^2 = 1$ signifying that the model/regression-line perfectly fits the data [9].

2.3.2 Pattern search

Finding the maxima or minima (collectively known as extrema) of a first order single variable function can easily be found by equating the derivative of this function to zero. However finding the derivative of certain functions is not always easy or possible. In such conditions, various search techniques are used to find the maxima or minima in a uni-modal (a uni-modal function contains only one minimum or maximum on the specified interval) continuous function over an interval without using derivatives [26]. Golden section search algorithm is one such search method. The algorithm derives its name from the Golden ratio (0.61803...)

Two numbers are said to be in the Golden ratio if their ratio is same as the ratio of their sum to the larger of the two quantities. Assuming $\beta > \alpha$ then this can be expressed as[11]:

$$\frac{\alpha+\beta}{\beta} = \frac{\beta}{\alpha} = \phi \tag{2.17}$$

where ϕ is the Golden ratio whose value is given by:

$$\phi = \frac{\sqrt{5}-1}{2} = 0.61803398874989...... \tag{2.18}$$

Assuming *f(x)* to be an uni-modal function in the intervals between *a* and *b*. It is very important for the extrema exists within the range to prevent misleading results. The maxima is represented by $f(P_{max})$ such that $a \leqslant P_{max} \leqslant b$.

- Points P_1&P_2 are chosen such that they satisfy:

$$P_1 = a + (1-\phi)(b-a) \tag{2.19}$$

$$P_2 = a + \phi(b-a) \tag{2.20}$$

- $f(a)$,$f(P_1)$,$f(P_2)$ and $f(b)$ is computed.
- If $f(P_1) > f(P_2)$ then the outer bound is discarded and replaced by P_2 and P_2 replaced P_1; a new P_1 is calculated using equation 2.19.
- Else the lower bound is cast-off to be replaced with P_1 and P_1 is swapped with P_2; with P_2 found afresh using equation 2.20.
- New values of either $f(P_1)$ or $f(P_2)$ are found out depending on the branch taken.
- The process repeated over and over again only stopping when either the iteration count has run out or if the lower and upper bounds are close enough to be acceptably small.

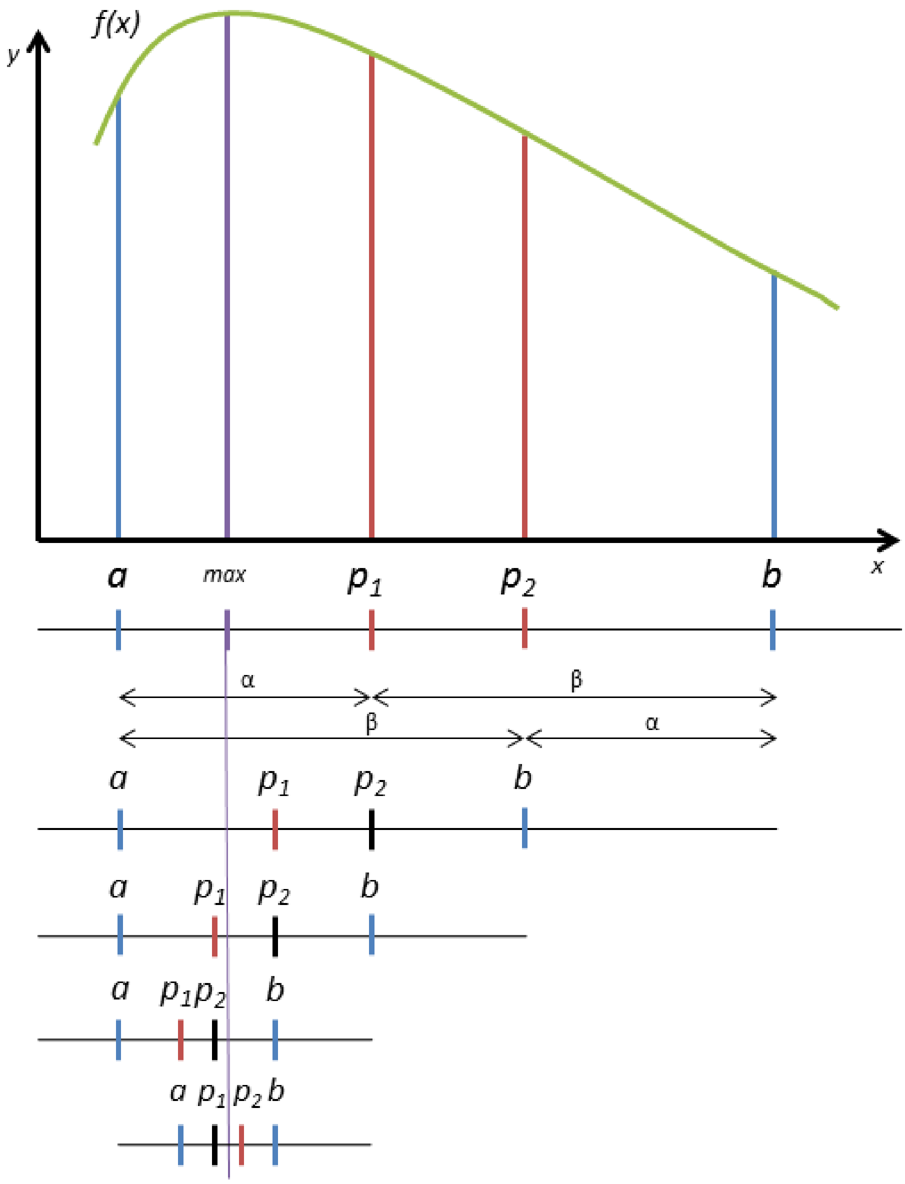

Figure 2.14: Golden Section search algorithm

The advantage of using Golden search over other search methods is that the extrema is found in the least number of steps and every iteration requires only one additional data point. Thereby greatly reducing the complexity of the algorithm and hence the computation power and/or time required to lock-in onto the extrema.

- The blue points represent extremes of the successive
- Red points are the newly evaluated values
- Black points are the already evaluated values.

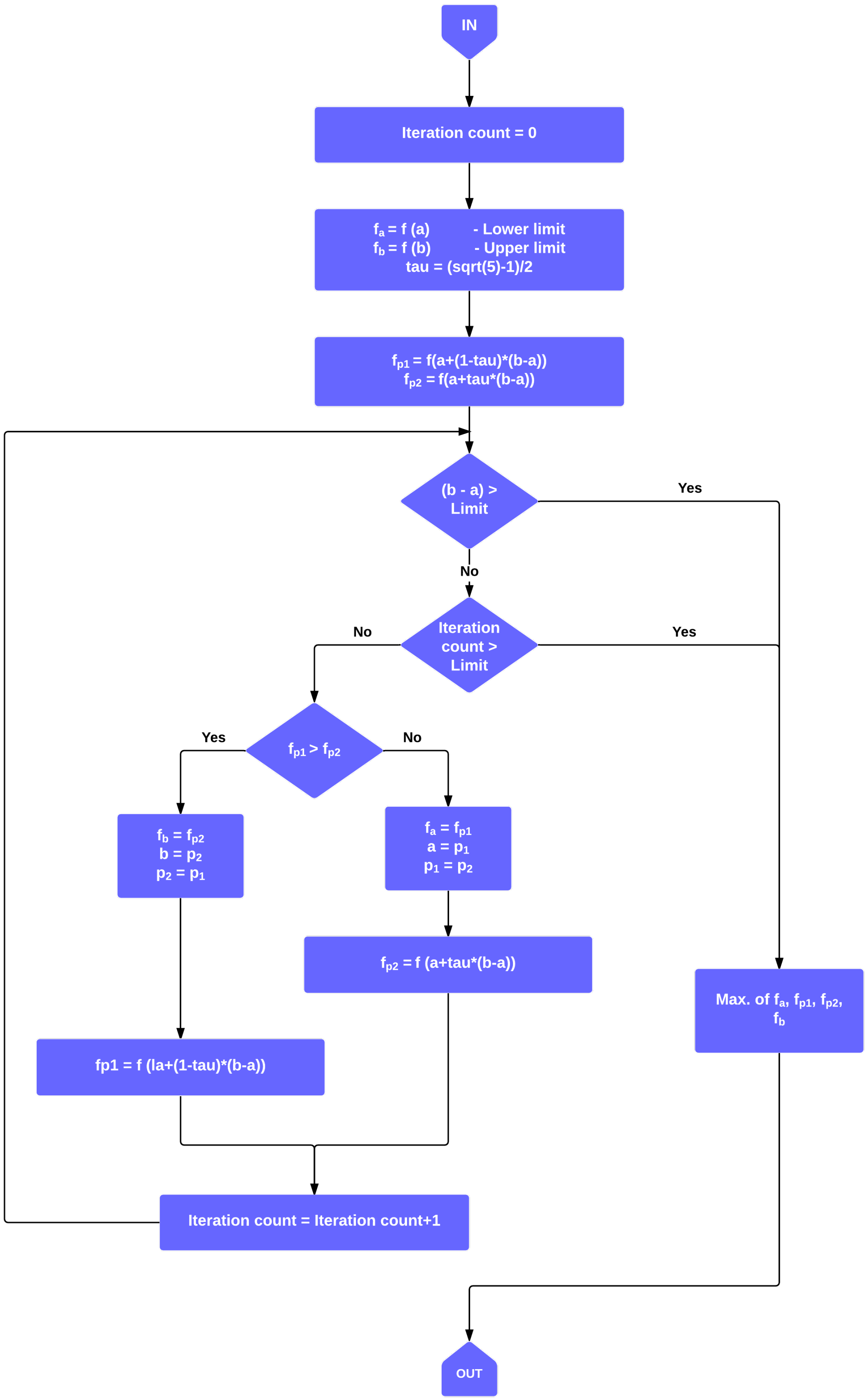

Figure 2.15: Golden Section search algorithm (modified from [30])

3 DESIGN AND IMPLEMENTATION

This chapter covers the implementation details of the concept, the algorithms. All the simulations were first carried out in MATLAB® and Simulink®, testing and verifying.The section also introduces the proposed hybrid algorithm.

3.1 CELL CHARACTERISATION

In this section, Model of two types of cells (a-Si and DSCs) is discussed.There are several Models that have been analysed in literature which are usually variations of the Single Diode model or the Double Diode model (discussed in section 2.1.1,2.1.2 and 2.1.3).

3.1.1 Test Setup

In the pursuance of creating a working solar cell model and to validate the algorithm several measurements would need to be performed. The Test-rig consisted of a blacked out enclosure to suppress interference from ambient light. The Test-rig or Light-box is fitted with an array of evenly spaced White-Light Emitting Diode (LED)s to provide uniform illumination on the Test subject. The LED-array are calibrated and temperature controlled so as to provide white light with a known spectra. A high precision Lux Meter(*GOSSEN Mavolux 5032B*) is used to measure the intensity of the light, as perceived by the human eye. The *GOSSEN* serves as a reference for Lux measurement throughout the project. The Light chamber is also routinely calibrated against a reference cell to factor-in the variations and degradation of the LEDs. The intensity of light is varied using a High-Voltage power source. A pictorial representation of the above description can be seen is figure 3.1 on page 28.

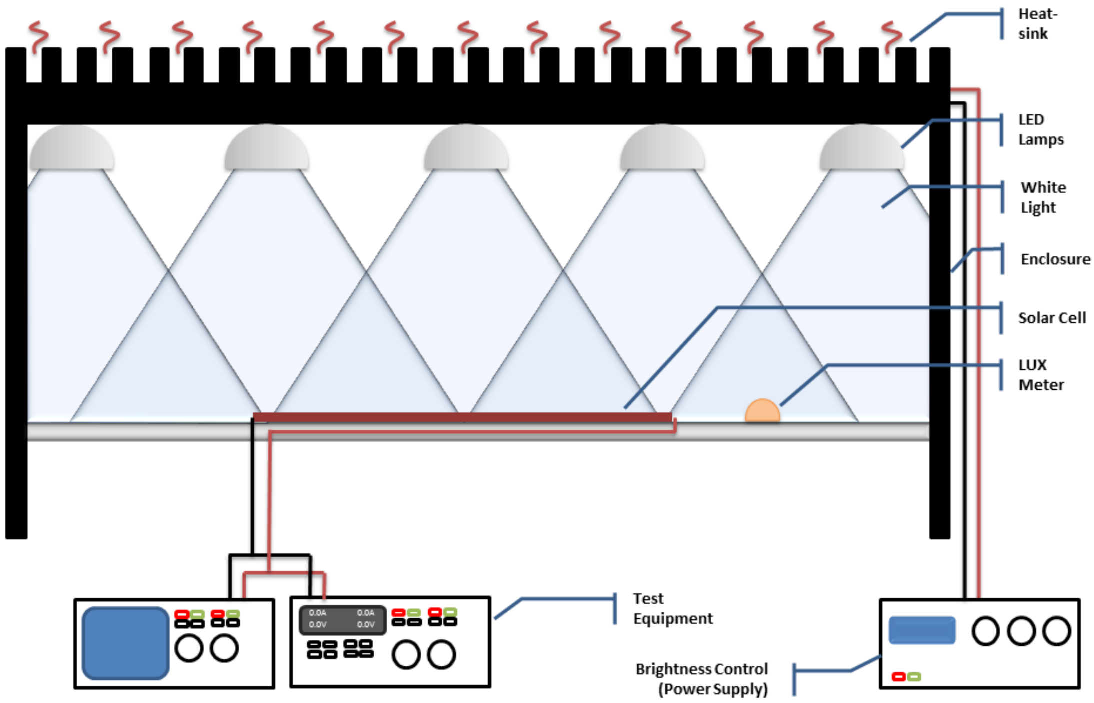

Figure 3.1: Test Setup

Electrical models for solar cells are frequently found in literature [31] and [33] among others -discussed in section 2.1.1 to 2.1.3.However DSCs come in may different flavours:- dissimilar electrolytes & electrodes; additional layers and junctions. Added to this fact, due to the near impossibility of accurately measuring the multitude of variables of a unknown cell, for this research work, a model was constructed by placing a the test cell under a battery of varied illuminations (0 Lux - 5050 Lux) shown in figure 3.2. Which resulted in a surface that closely resembles the cell's operation under real world conditions. Particular attention was paid to low light conditions which is to be expected for indoor illuminations ($<$ 2000 Lux).As DSCs display are very stable output across temperature ranges found indoor [19], the above model was made independent of temperature variations.

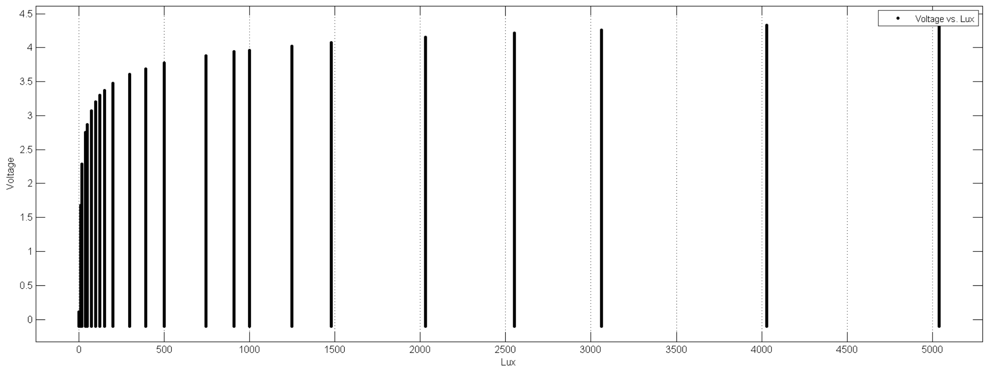

Figure 3.2: Spread of measured Illumination vs Voltage

The Cell-under-test is connected to a Source-Measure Unit (SMU). SMUs have flexibility in their outputs, to be classified as having four-quadrant outputs, it must be able to source power as well as sink power. Sourcing power refers to providing the stimulus for a circuit, and sinking power refers to dissipating power that is being applied by an external active component such as a battery, a charged capacitor, or another power source [16] - a solar cell in our case.

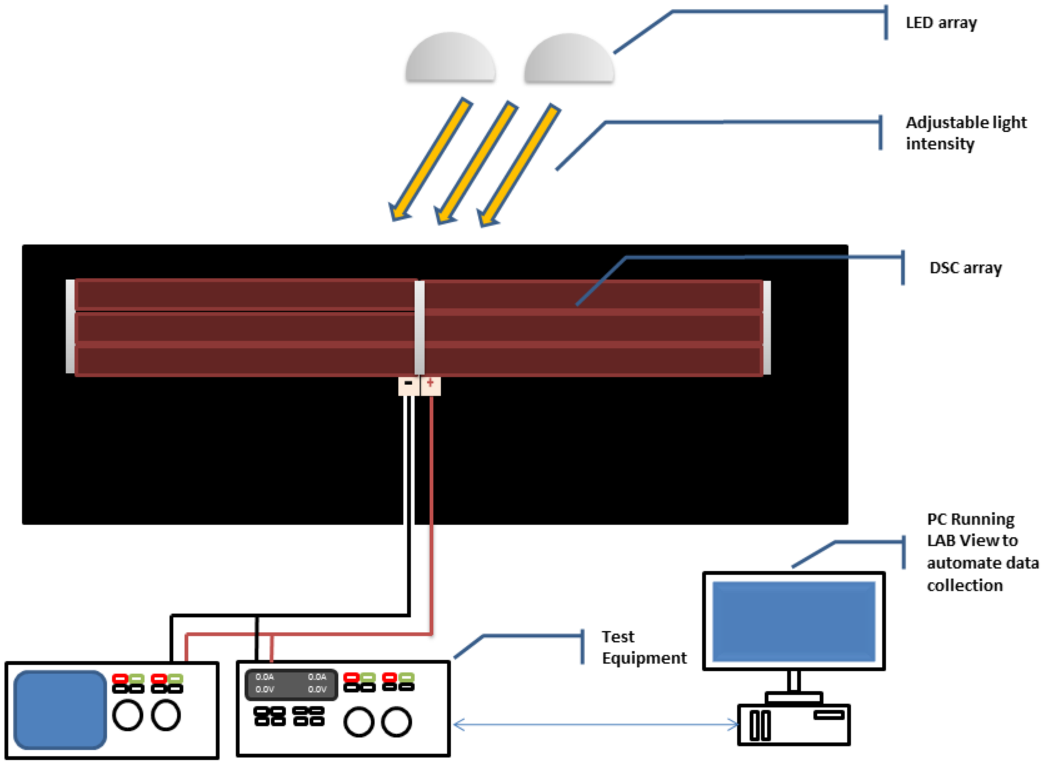

Figure 3.3: Cell Characterisation

As the Sink potential is increased in tiny increments, starting from 0 V to V_{OC} and beyond, the cell is forced to operate at the Sink Voltage resulting in the I-V graph depicted in figure 3.4 on page 30. When the above is repeated for several different light intensities we get a three-dimensional surface shown in figure 3.5 on page 31.Note that, V_{OC} is the maximum voltage available from a cell this occurs when the cell produces zero Current (when the graph intersects the x-axis).

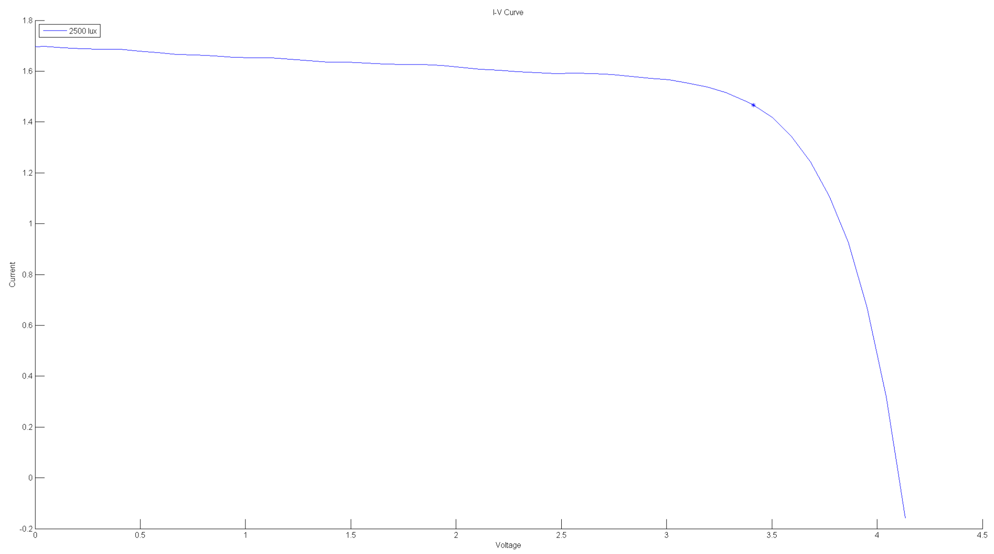

Figure 3.4: I-V curve for the array at steady illumination

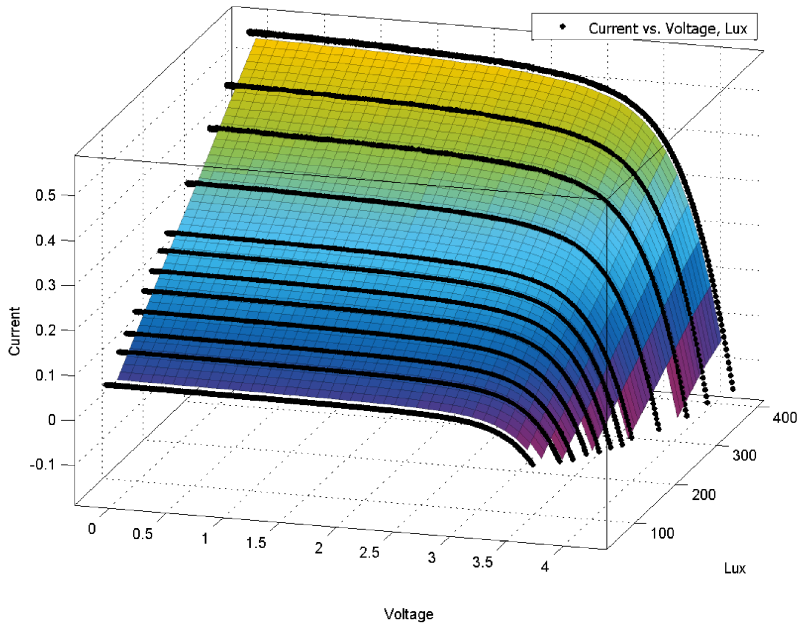

Figure 3.5: I-V curve for the array at varying illumination

3.2 MODELLING AND SIMULATIONS

The three-dimensional surface thus created in the section above acts as a function, a look-up table of sorts, for a given illumination and voltage; the function computes a appropriate value for the cell's current . ** to convert continuous voltage values to discreet values **,a transfer functions are used. The DSCs subsystem is represented in the figure 3.6 below. Capacitor is added in order to accurately mimic the response of DSCs under test as discussed in 2.1.3. The diode acts as a Snubber, eliminating flyback across the inductive load. This sub-system is placed under a mask in the abstract view, shown in figure 3.7 on page 32, in order to simplify operation and for ascetic reasons. The validation of the said model is discussed in section 3.3. Another look-up table provides Open-circuit Voltages (V_{OC}) for a given Lux, to be used in certain algorithms.

The *Scopes and Outputs* subsection is used to plot data on to graphs and to push data onto Matlab, for further analysis.

The MPPT *Controller Block* (figure 3.8 on page 33) is modelled as a variant subsystem. The variant-control determines which variant is active, and is set before the simulation is started. This arrangement of subsystems makes it extremely easy to switch between and compare the various MPPT Algorithms without making any alterations to the rest of the model.

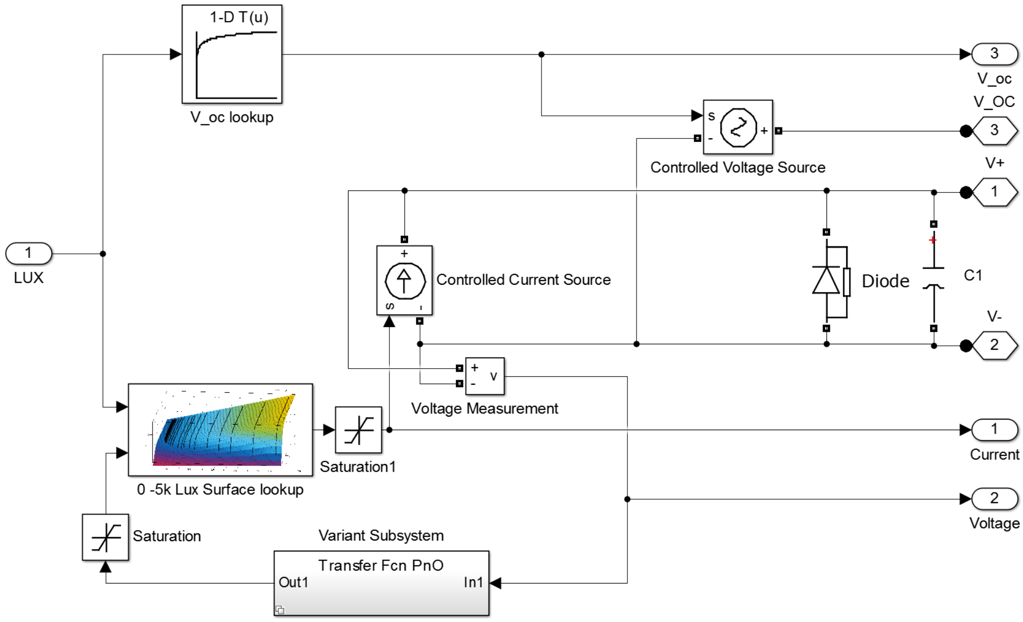

Figure 3.6: Modelling of the DSC Subsystem

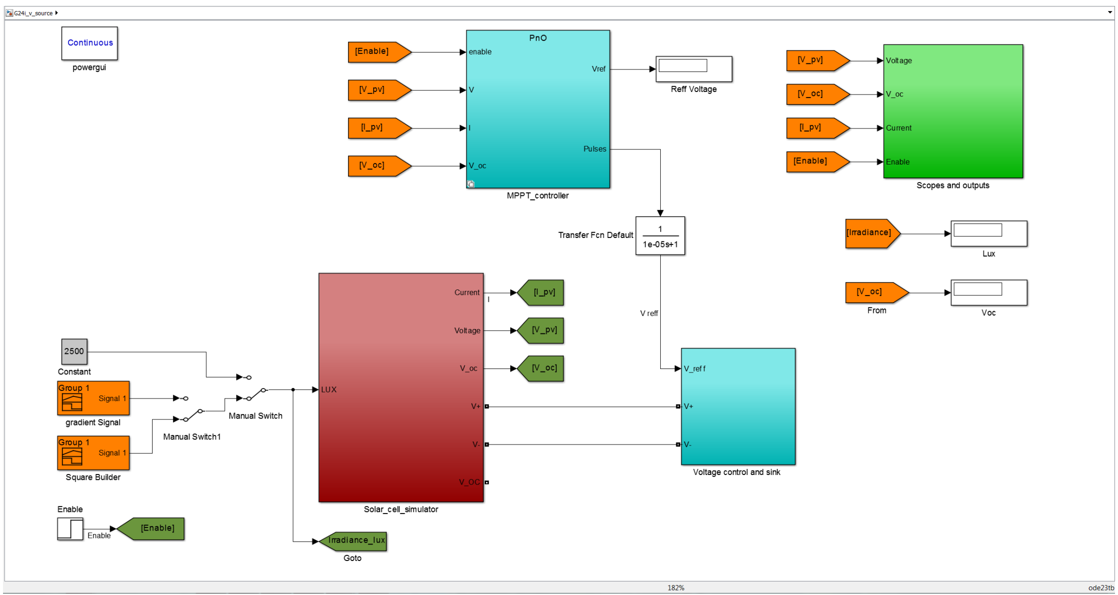

Figure 3.7: Top Model

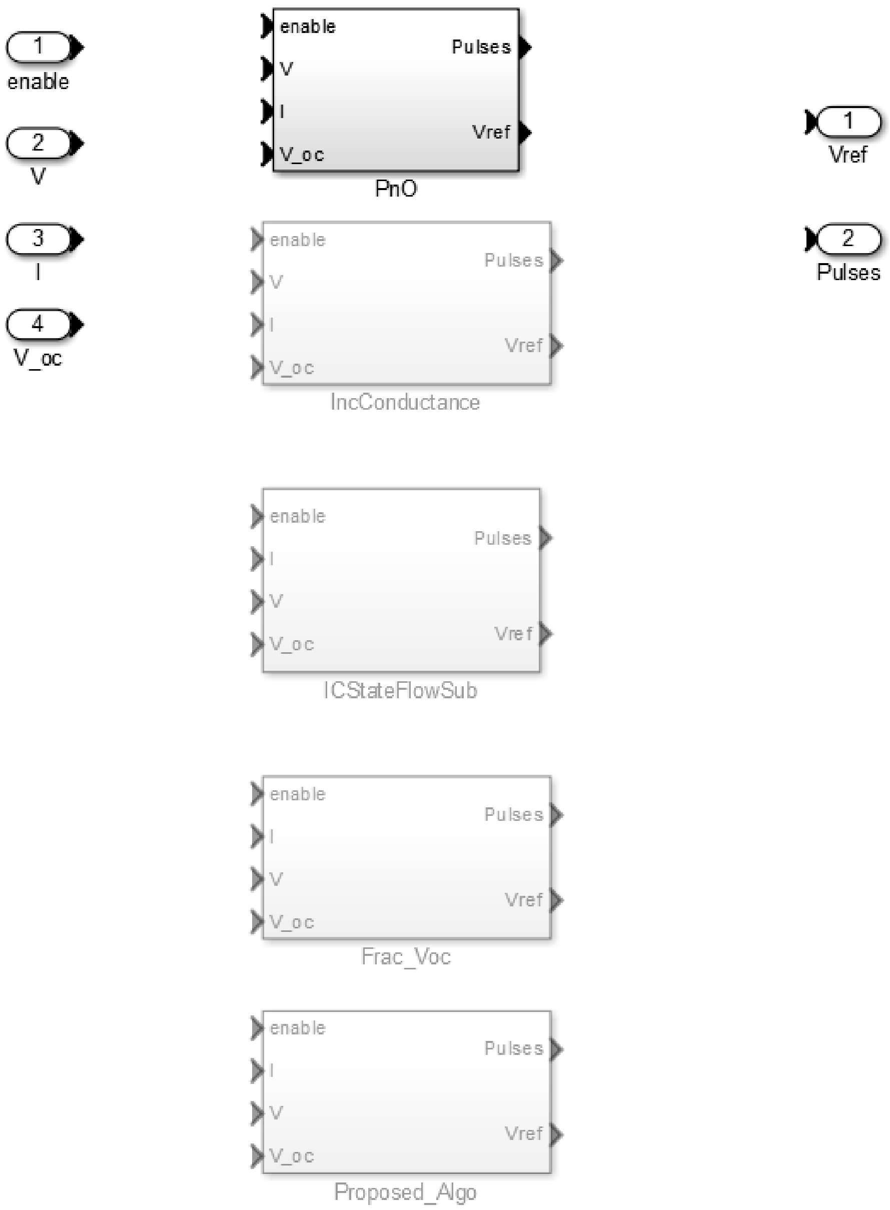

Figure 3.8: MPPT controller

3.3 VALIDATION OF THE MODEL IN MATLAB®

Since the credibility of the thesis rests on the accuracy of the model used to compare the different algorithms therefore, a section is devoted to the validation of the same. The easiest way to do this would be to compare the divergence of Matlab Model (Section:3.1) with the values obtained via experiment.

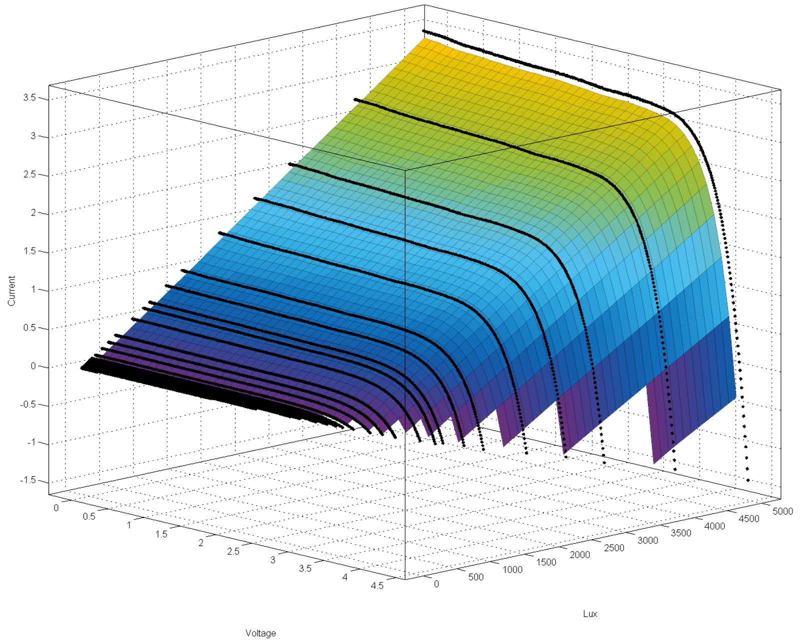

Figure 3.9: 3-D representation of the cell's characteristics measured in the lab

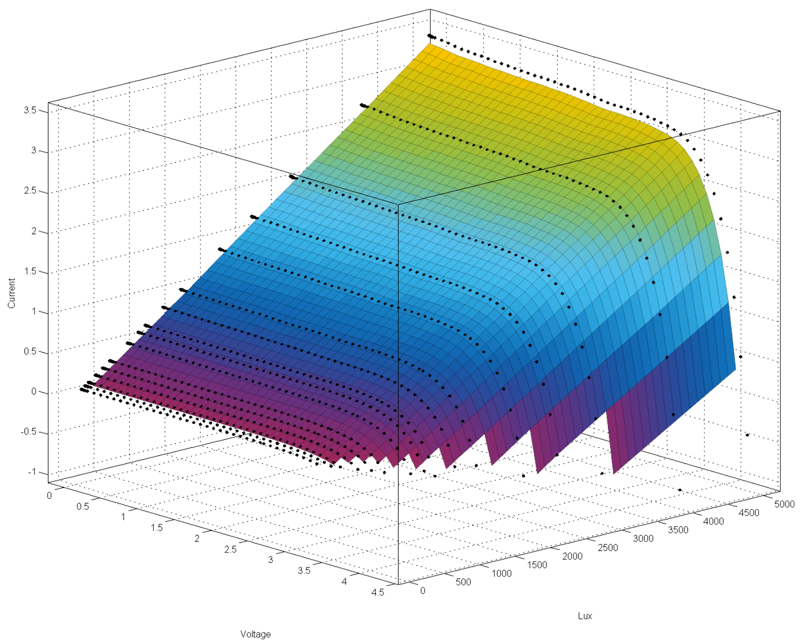

Figure 3.10: Surface generated by the Matlab model

The model depicted in figure 3.9 is generated using experimental data. Measurements were taken with a step size of 0.01V compared to the 0.1V step size for the simulated model, as is evident in the figures.The larger step size makes for faster calculations and smaller lookup tables. A fair bit of Interpolation is utilized to estimate values for points in between however, as proved below these estimation do not introduce any significant errors into the model.

On the Subtraction of one surface from the other, we are left with figure 3.11. This resulting 3-Dimensional surface represents the degree by which the two models are different. Figure 3.12 on page 36 illustrates this variation in the form of a contour map, in which majority of the discrepancy lies within the error margin of 0.1 mA and the divergence in the area of operation and of interest (0 - 4 V) is significantly less. This goes to prove the model used in the simulation behaves as close to possible to a real DSCs under test conditions.

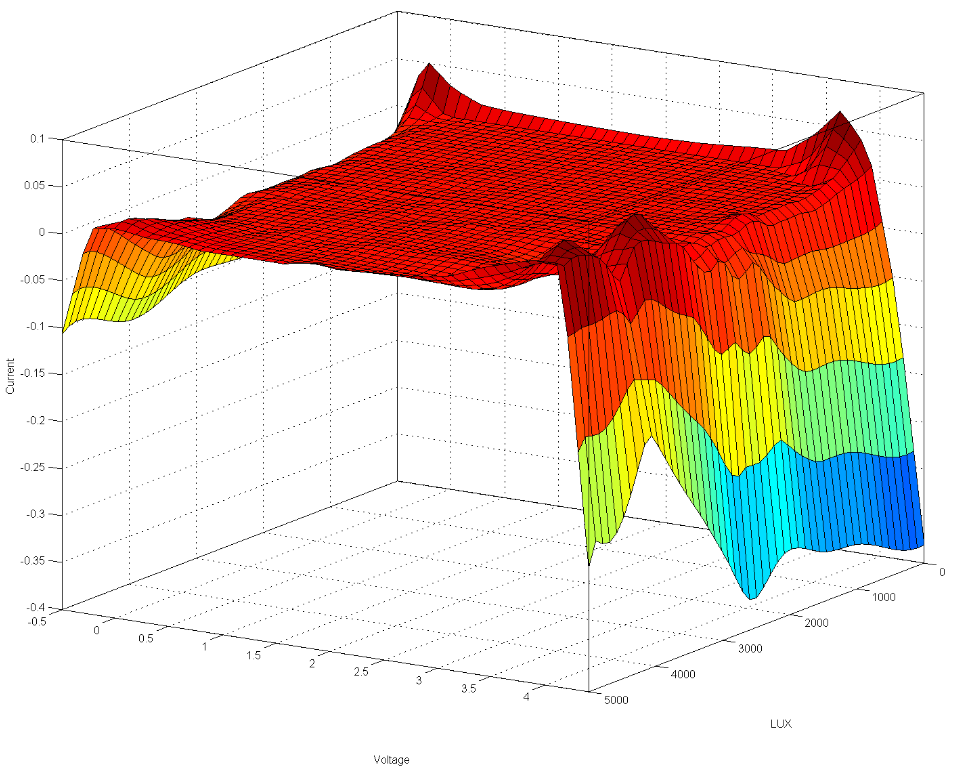

Figure 3.11: Model resulting from the difference of the two models (Figures 3.9 & 3.10)

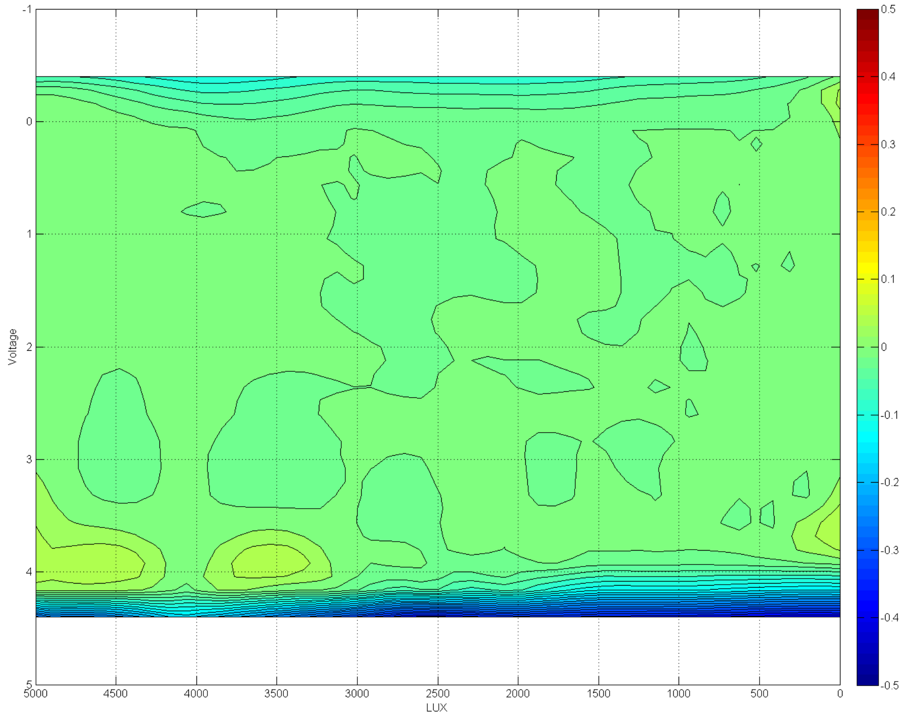

Figure 3.12: Contour map of the difference

3.4 PROPOSED METHOD

[15]

This work presents an experimental comparison; Using four identical PV, under strictly the same set of technical and meteorological conditions, an experimental comparison of four most used MPPT methods for PV power systems is done.This comparison shows the advantage of use of a MPPT with a variable tracking step.

[17] This paper presents a new algorithm for tracking maximum power point in photovoltaic systems. This is a fast tracking algorithm, where an initial approximation of MPP quickly achieved using a variable step-size. Subsequently, the exactMPP can be targeted using any conventional method like the hill-climbing or incremental conductance method. Thus, the drawback of a fixed small step-size over the entire tracking range is removed, resulting in reduced number of iterations and much faster tracking compared to conventional methods.
My implementation draws inspiration for the above article for its two-stage algorithm to reduce the number of iterations but deviates significantly in the implementation and algorithms used to identify the MPP

[20]

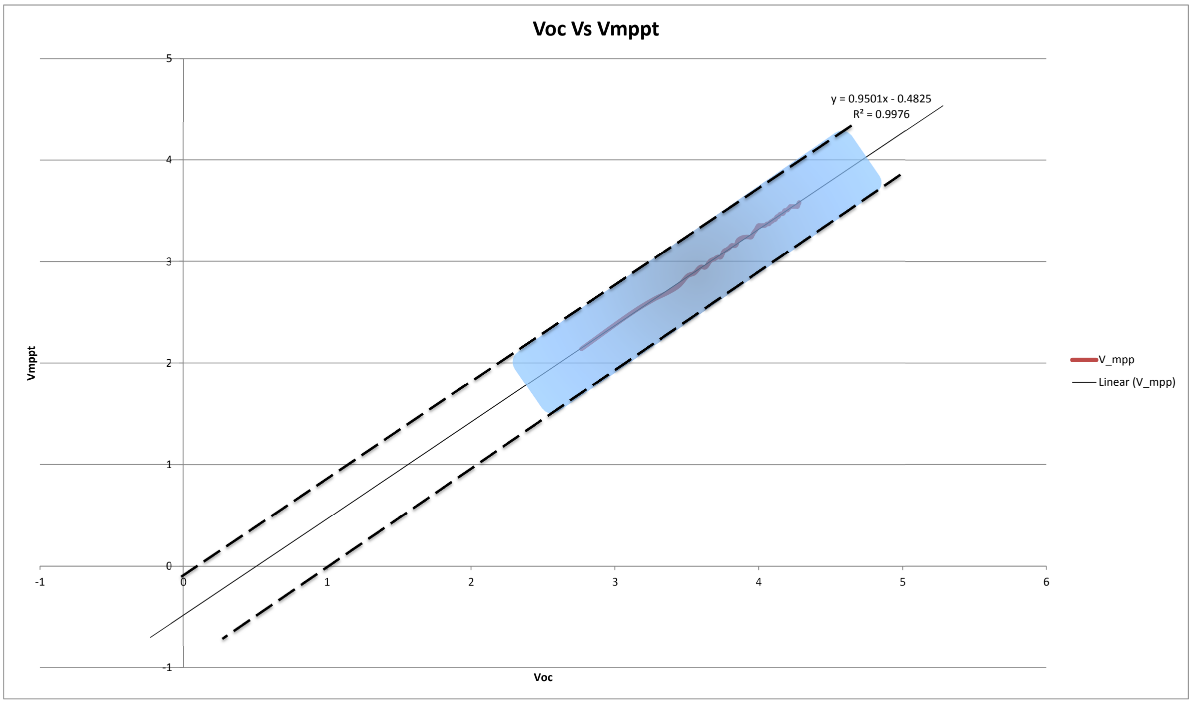

Figure 3.13: Probability field

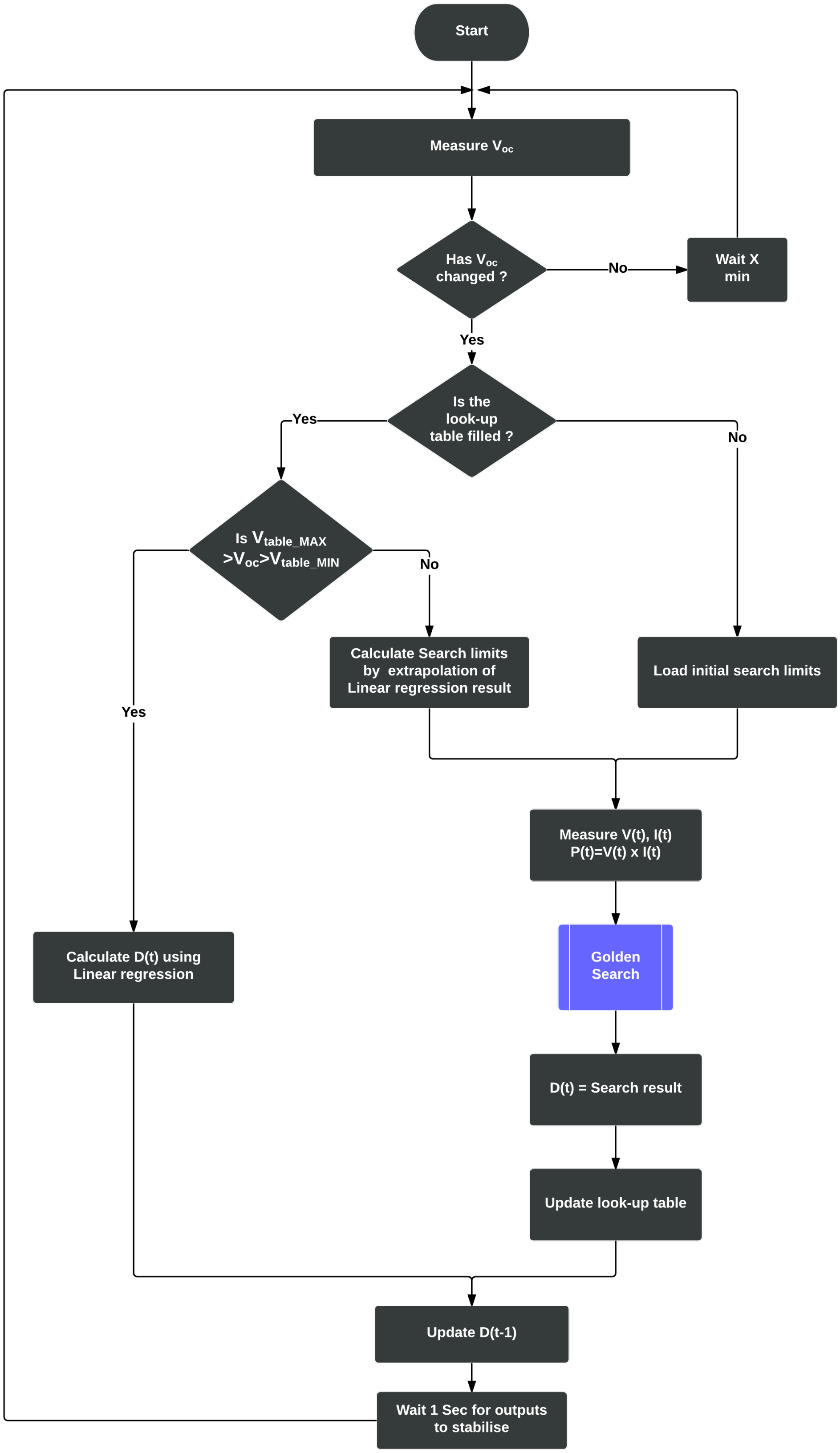

Figure 3.14: Flow chart for Proposed MPPT Algorithm

4 RESULT DISCUSSION

4.1 PERTURB AND OBSERVE METHOD

insert text here insert text here

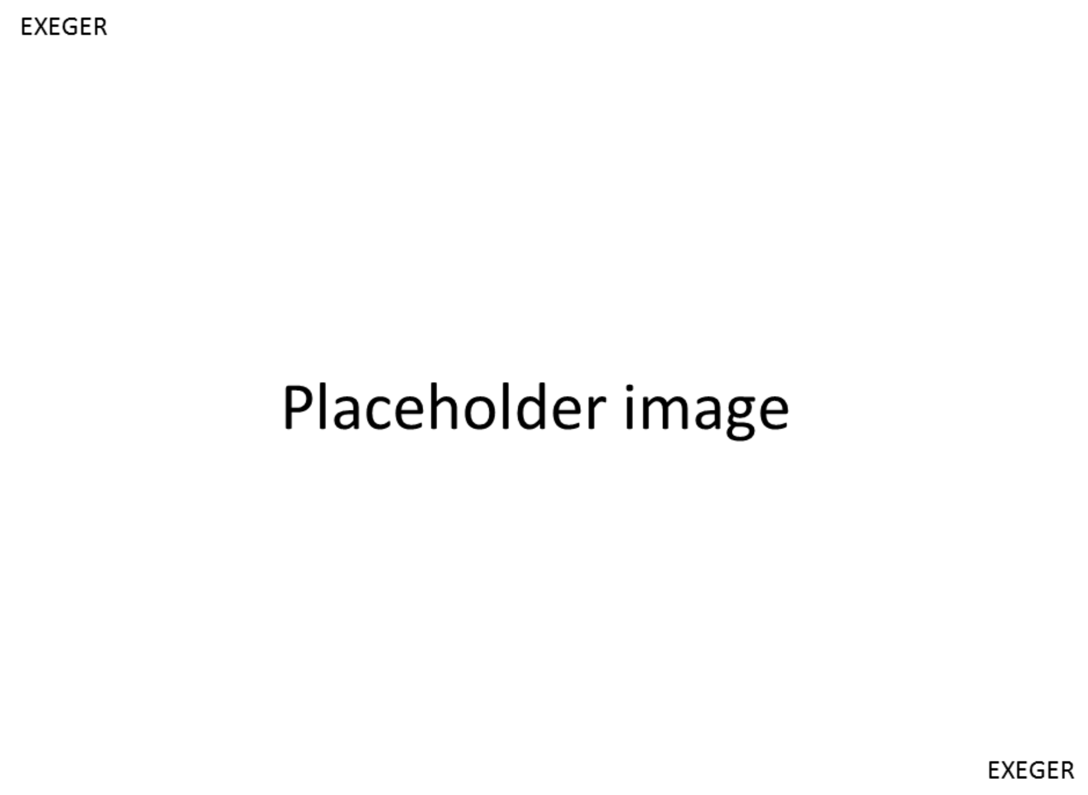

Figure 4.1: Perturb and Observe Method on implementation

4.2 INCREMENTAL CONDUCTANCE METHOD

insert text here insert text here.

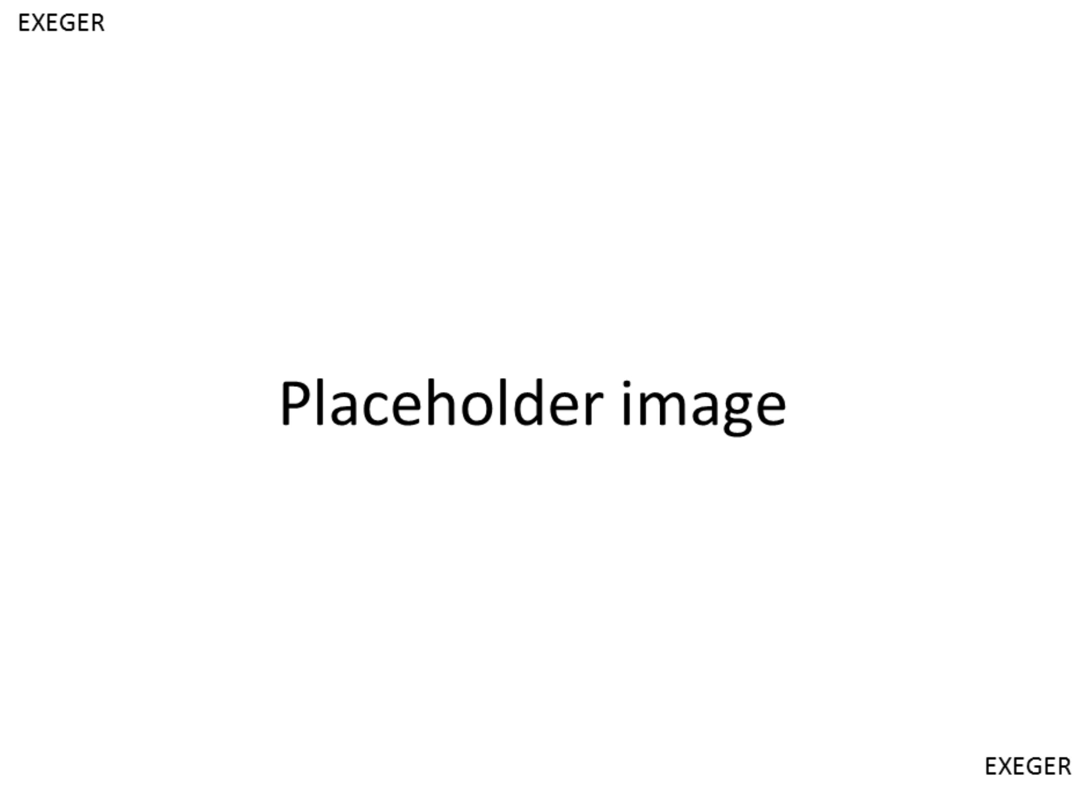

Figure 4.2: Incremental Conductance Method on implementation

4.3 FRACTIONAL OPEN CIRCUIT VOLTAGE METHOD

insert text here insert text here.

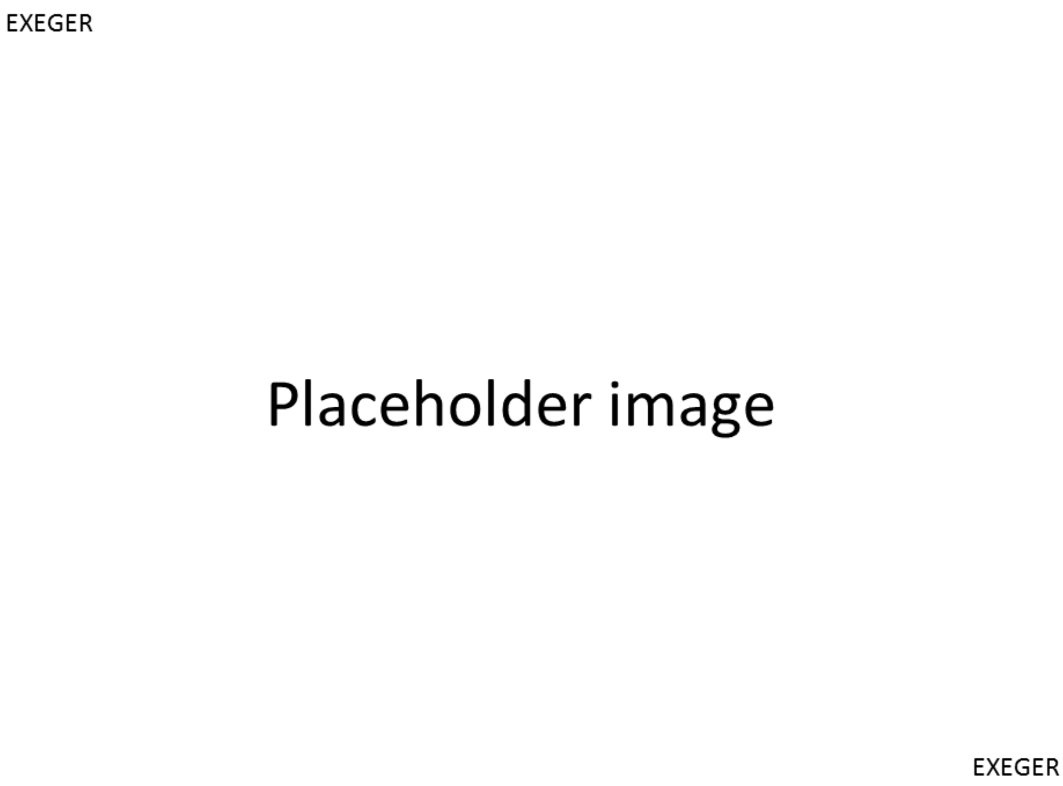

Figure 4.3: Fractional Open Circuit Voltage on implementation

4.4 PROPOSED METHOD

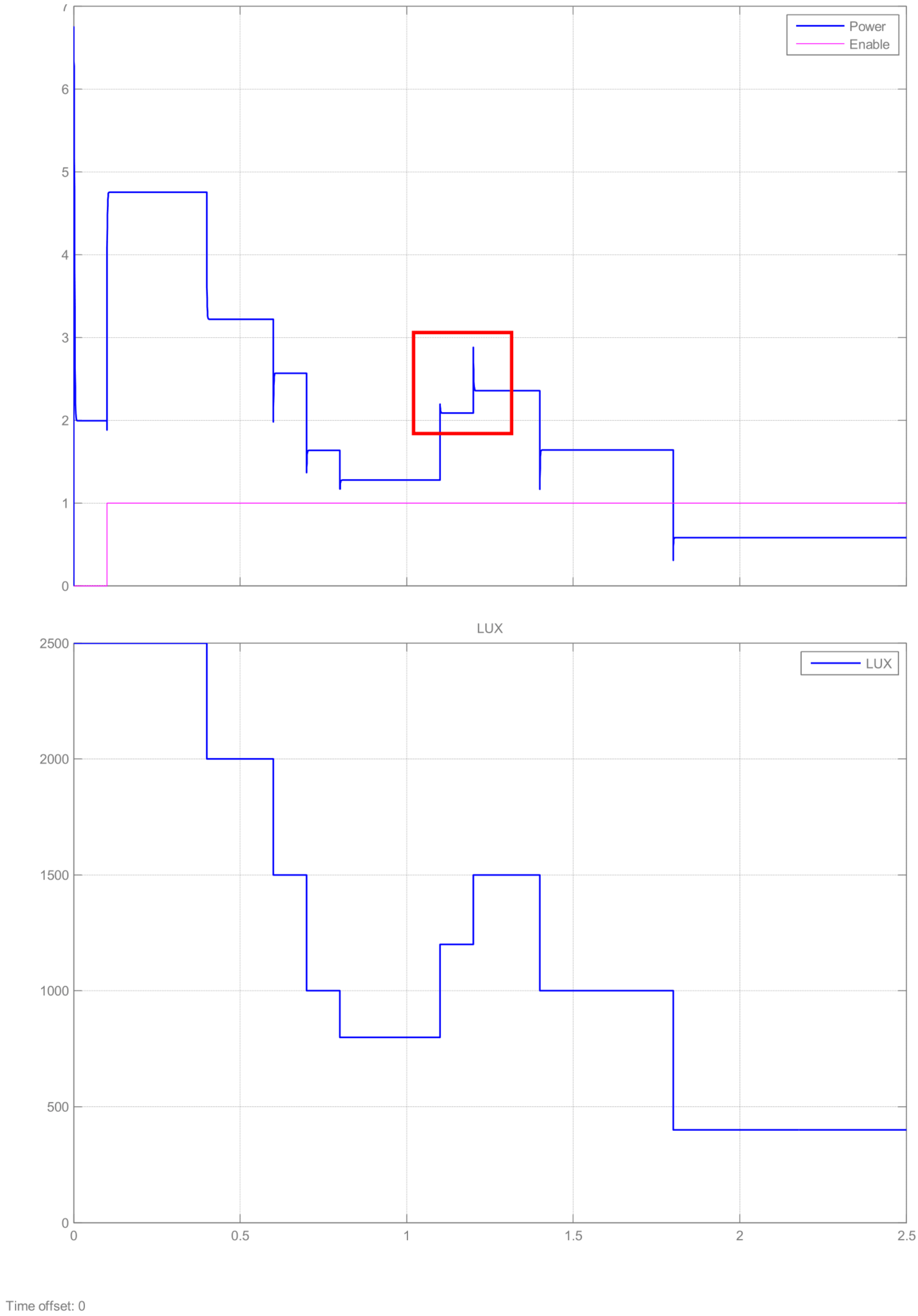

Figure 4.4: fractional open circuit voltage on implementation

5 CONCLUSION AND FUTURE WORK

This final chapter concludes the results obtained from the thesis and attempts to give direction for the future work in this area.

While several MPPT algorithms where studied in relation to this thesis , three of the most common ones were selected to be tested in this thesis. It was observed that each of the selected algorithms had one or more shortcoming when implemented on DSCs

5.0.1 **text**[15]

Houssamo, Issam, Fabrice Locment, and Manuela Sechilariu. "*Experimental analysis of impact of MPPT methods on energy efficiency for photovoltaic power systems.*" International Journal of Electrical Power & Energy Systems 46 (2013): 98-107.

This work presents an experimental comparison; Using four identical PV, under strictly the same set of technical and meteorological conditions, an experimental comparison of four most used MPPT methods for PV power systems is done.This comparison shows the advantage of use of a MPPT with a variable tracking step.

5.0.2 **text**[17]

Jain, Sachin, and Vivek Agarwal. "*A new algorithm for rapid tracking of approximate maximum power point in photovoltaic systems.*" Power Electronics Letters, IEEE 2.1 (2004): 16-19.

This paper presents a new algorithm for tracking maximum power point in photovoltaic systems. This is a fast tracking algorithm, where an initial approximation of MPP quickly achieved using a variable step-size. Subsequently, the exactMPP can be targeted using any conventional method like the hill-climbing or incremental conductance method. Thus, the drawback of a fixed small step-size over the entire tracking range is removed, resulting in reduced number of iterations and much faster tracking compared to conventional methods.

My implementation draws inspiration for the above article for its two-stage algorithm to reduce the number of iterations but deviates significantly in the implementation and algorithms used to identify the MPP

5.0.3 **text**[20]

Liu, Yi-Hua, and Jia-Wei Huang. "*A fast and low cost analog maximum power point tracking method for low power photovoltaic systems.*" Solar Energy 85.11 (2011): 2771-2780.

**add TEXT important RESEARCH *

Typically, MPPT methods utilized in medium and high power PV systems uses measured cell characteristics (current, voltage, power) along with an online search algorithm to compute the corresponding MPP. Due to the complexity of the required mathematical operations, a Digital Signal Processor (DSP) or a relatively powerful micro-controller is typically needed, which increases the cost of the system.Moreover, it consumes significant portion of the generated power. Therefore, aMPPT circuit with low-cost and fast-tracking features is essential .

It has already established that there exists a relation between V_{MPP} and V_{OC} in equation 2.12 and is famously used in the FOCV method. However we see that this does not hold true for all illumination conditions and certainly not for low-light(less than 1500 Lux) as compared to higher insolation. Since V_{OC} is is a logarithmic function of I_{ph}, the relationship between V_{MP} and I_{MP}.with respect to irradiation is not linear. However, it is possible to linearize this relationship for an interval where the value of V_{OC} is sufficiently insensitive to irradiation. That is, the Voltage approximation line (VAL) can be calculated as the tangent line of the MPP locus where the sensitivity of V_{OC} to I_{ph} is lower than a pre-defined threshold. This relationship is illustrated in Figure 5.1 on page 45.

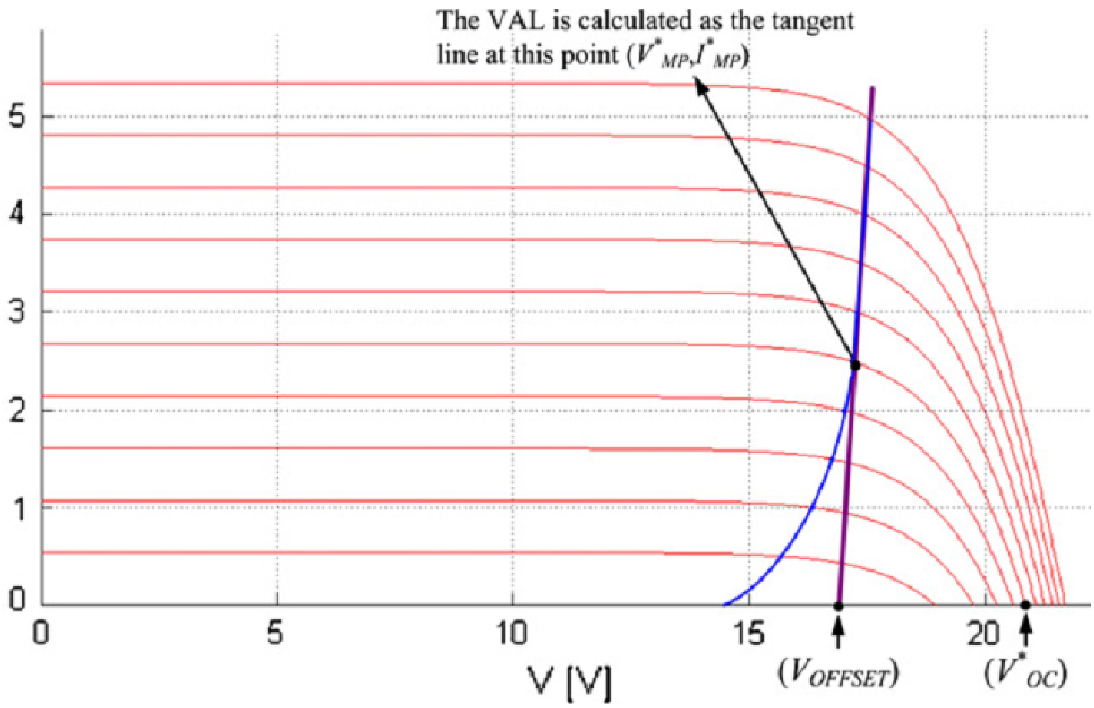

Figure 5.1: I–V curves of the solar panel under different irradiation levels and the voltage approximation line. [20]

The same trend can be seen on the I-V curves for the DSCs under test (Figure 5.2).

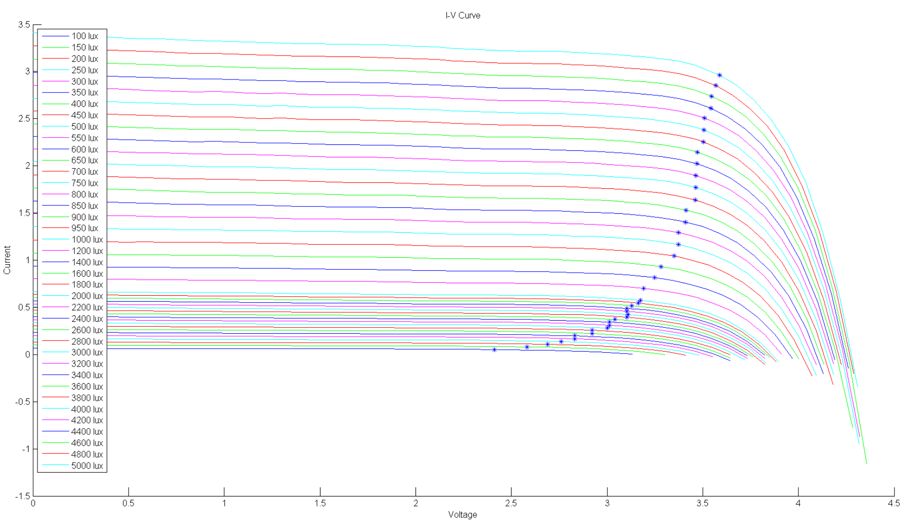

Figure 5.2: Variation of V_{MPP} for different illumination observed **in/on** the DSC under test

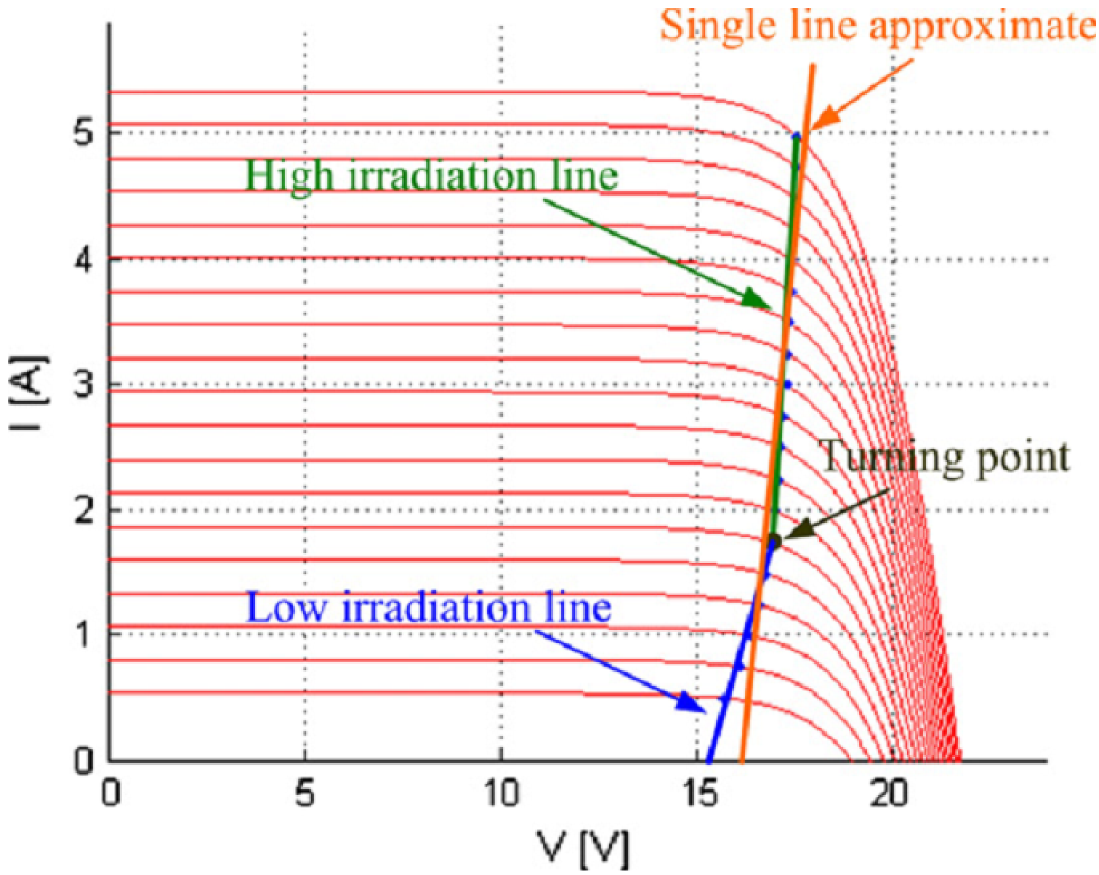

Figure 5.3: Research Cell Efficiency Records [20]

insert pictures

5.0.4 **text**[4]

Dondi, Denis, et al. "*Modeling and optimization of a solar energy harvester system for self-powered wireless sensor networks.*" Industrial Electronics, IEEE Transactions on 55.7 (2008): 2759-2766.

**Initial modelling strategies where based on this paper, improving the efficiency. # discrete components# **

5.0.5 **text**[1]

Chu, Chen-Chi, and Chieh-Li Chen. "*Robust maximum power point tracking method for photovoltaic cells: A sliding mode control approach.*" Solar Energy 83.8 (2009): 1370-1378.

5.0.6 **text**[29]

** Write about this in the proposed algo part** Urayai, Caston, and G. Amaratunga. "*Single sensor boost converter-based maximum power point tracking algorithms.*" Applied Power Electronics Conference and Exposition (APEC), 2011 Twenty-Sixth Annual IEEE. IEEE, 2011.

Two new maximum power point tracking algorithms are presented: the input voltage sensor, and duty ratio maximum power point tracking algorithm (ViSD algorithm); and the output voltage sensor, and duty ratio maximum power point tracking algorithm (VoSD algorithm).unlike the incremental conductance algorithm which requires two sensors (the voltage sensor and current sensor), the two algorithms are more desirable because they require only one sensor: the voltage sensor.

5.0.7 **text**[2]

Clark, C., and A. Lopez. "*Power system challenges for small satellite missions.*" Proceedings of the 2006 Small Satellites, Systems and Services Symposium, D. Danesy, Ed. The Netherlands: ESA. 2006.

TExt Inspiration for use of multiple power buses

BIBLIOGRAPHY

[1] C.-C. Chu and C.-L. Chen. "Robust maximum power point tracking method for photovoltaic cells: A sliding mode control approach". In: *Solar Energy* 83.8 (2009), pp. 1370–1378 (cit. on p. 46).

[2] C. Clark and A. Lopez. "Power system challenges for small satellite missions". In: *Proceedings of the 2006 Small Satellites, Systems and Services Symposium, D. Danesy, Ed. The Netherlands: ESA*. 2006 (cit. on p. 47).

[3] L. G. Connelly and A. E. Bair. "Discrete Event Simulation of Emergency Department Activity: A Platform for System-level Operations Research". In: *Academic Emergency Medicine* 11.11 (2004), pp. 1177–1185 (cit. on p. 21).

[4] D. Dondi et al. "Modeling and optimization of a solar energy harvester system for self-powered wireless sensor networks". In: *Industrial Electronics, IEEE Transactions on* 55.7 (2008), pp. 2759–2766 (cit. on pp. 6, 46).

[5] M. A. Eltawil and Z. Zhao. "MPPT techniques for photovoltaic applications". In: *Renewable and Sustainable Energy Reviews* 25 (2013), pp. 793–813 (cit. on pp. 5, 15).

[6] J. Enrique, J. Andújar, and M. Bohórquez. "A reliable, fast and low cost maximum power point tracker for photovoltaic applications". In: *Solar Energy* 84.1 (2010), pp. 79–89 (cit. on pp. 3, 4).

[7] T. Esram and P. L. Chapman. "Comparison of photovoltaic array maximum power point tracking techniques". In: *IEEE TRANSACTIONS ON ENERGY CONVERSION EC* 22.2 (2007), p. 439 (cit. on pp. 5, 15, 22).

[8] R. Faranda and S. Leva. "Energy comparison of MPPT techniques for PV Systems". In: *WSEAS transactions on power systems* 3.6 (2008), pp. 446–455 (cit. on p. 15).

[9] J. Frost. *Regression Analysis: How Do I Interpret R-squared and Assess the Goodness-of-Fit?* May 30, 2013. URL: http://blog.minitab.com/blog/adventures-in-statistics/regression-analysis-how-do-i-interpret-r-squared-and-assess-the-goodness-of-fit (visited on 11/03/2014) (cit. on p. 22).

[10] GCell. *How does DSSC work*. URL: http://gcell.com/wp-content/uploads/DSSC_cycle.jpg (visited on 10/03/2014) (cit. on p. 10).

[11] P. E. Gill, W. Murray, and M. H. Wright. *Practical optimization*. Academic Press, 1981 (cit. on p. 23).

[12] S. Gomathy, S. Saravanan, and S. Thangavel. "Design and implementation of maximum power point tracking (MPPT) algorithm for a standalone PV system". In: *International Journal of Scientific & Engineering Research* 3.3 (2012), pp. 1–7 (cit. on p. 17).

[13] M. Grätzel. "Conversion of sunlight to electric power by nanocrystalline dye-sensitized solar cells". In: *Journal of Photochemistry and Photobiology A: Chemistry* 164.1 (2004), pp. 3–14 (cit. on p. 1).

[14] C. Honsberg. *Double Diode Model*. URL: `http://pveducation.org/pvcdrom/characterisation/double-diode-model` (visited on 11/03/2014) (cit. on pp. 12, 13).

[15] I. Houssamo, F. Locment, and M. Sechilariu. "Experimental analysis of impact of MPPT methods on energy efficiency for photovoltaic power systems". In: *International Journal of Electrical Power & Energy Systems* 46 (2013), pp. 98–107 (cit. on pp. 36, 43).

[16] N. Instruments. *What Is a Source Measure Unit*. Feb. 19, 2014. URL: `http://www.ni.com/white-paper/6850/en/` (visited on 11/23/2014) (cit. on p. 29).

[17] S. Jain and V. Agarwal. "A new algorithm for rapid tracking of approximate maximum power point in photovoltaic systems". In: *Power Electronics Letters, IEEE* 2.1 (2004), pp. 16–19 (cit. on pp. 36, 43).

[18] K. Kalyanasundaram. *Dye-sensitized solar cells*. EPFL press, 2010 (cit. on p. 1).

[19] H.-S. Lee et al. "A high temperature stable electrolyte system for dye-sensitized solar cells". In: *Electrochimica Acta* 55.24 (2010), pp. 7159–7165 (cit. on p. 28).

[20] Y.-H. Liu and J.-W. Huang. "A fast and low cost analog maximum power point tracking method for low power photovoltaic systems". In: *Solar Energy* 85.11 (2011), pp. 2771–2780 (cit. on pp. 37, 44–46).

[21] S. Marsland. *Machine learning: an algorithmic perspective*. CRC Press, 2011 (cit. on p. 21).

[22] A. Messai, A. Mellit, A. Guessoum, and S. Kalogirou. "Maximum power point tracking using a GA optimized fuzzy logic controller and its FPGA implementation". In: *Solar energy* 85.2 (2011), pp. 265–277 (cit. on p. 20).

[23] M. S. Ngan and C. W. Tan. "A study of maximum power point tracking algorithms for stand-alone photovoltaic systems". In: *Applied Power Electronics Colloquium (IAPEC), 2011 IEEE*. IEEE. 2011, pp. 22–27 (cit. on pp. 5, 15, 19).

[24] NREL. *National Center for Photovoltaics, Research Cell Efficiency Records*. URL: `http://www.nrel.gov/ncpv/images/efficiency_chart.jpg` (visited on 09/23/2014) (cit. on p. 2).

[25] A. Reza Reisi, M. Hassan Moradi, and S. Jamasb. "Classification and comparison of maximum power point tracking techniques for photovoltaic system: A review". In: *Renewable and Sustainable Energy Reviews* 19 (2013), pp. 433–443 (cit. on pp. 6, 15, 20, 22).

[26] M. C. Seiler and F. A. Seiler. "Numerical recipes in C: the art of scientific computing". In: *Risk Analysis* 9.3 (1989), pp. 492–495. URL: `http://apps.nrbook.com/empanel/index.html#pg=492` (visited on 10/02/2014) (cit. on p. 23).

[27] J. Templin. "Chapter 1 : Linear Regression With One Predictor Variable". Oct. 24, 2006. URL: http://jonathantemplin.com/files/glm1/psyc790f06_lecture13.pdf (visited on 10/02/2014) (cit. on p. 21).

[28] M. Toivola et al. "Dye-sensitized solar cells on alternative substrates". In: (2010) (cit. on pp. 1, 10).

[29] C. Urayai and G. Amaratunga. "Single sensor boost converter-based maximum power point tracking algorithms". In: *Applied Power Electronics Conference and Exposition (APEC), 2011 Twenty-Sixth Annual IEEE*. IEEE. 2011, pp. 1238–1243 (cit. on p. 47).

[30] T. A. Van Wormer and D. L. Weiss. "Fitting Parameters to Complex Models by Direct Search". In: *Journal of Marketing Research* (1970), pp. 503–512 (cit. on p. 25).

[31] S. Vignati. "Solutions for Indoor Light Energy Harvesting". In: (2012) (cit. on pp. 11, 28).

[32] S. Wenger. "Strategies to optimizing dye-sensitized solar cells: organic sensitizers, tandem device structures, and numerical device modeling". PhD thesis. ÉCOLE POLYTECHNIQUE FÉDÉRALE DE LAUSANNE, 2010 (cit. on pp. 1, 11).

[33] V. Yong, S.-T. Ho, and R. P. Chang. "Modeling and simulation for dye-sensitized solar cells". In: *Applied Physics Letters* 92.14 (2008), pp. 143506–143506 (cit. on pp. 13, 14, 28).